Folding Bilateral Backstepping Output-Feedback Control Design For an Unstable Parabolic PDE

Stephen Chen *Student Member, IEEE*, Rafael Vazquez *Senior Member, IEEE*, and Miroslav Krstic *Fellow, IEEE*

***Abstract*— We present a novel methodology for designing output-feedback backstepping bilateral boundary controllers for an unstable 1-D diffusion-reaction partial differential equation with spatially-varying reaction. Using folding transforms the parabolic PDE into a 2×2 coupled PDE system with coupling through compatibility conditions. We apply a two-tiered backstepping approach, where the invertibility of the transformations guarantees the state-feedback controllers exponentially stabilize the trivial solution of the PDE system. A state observer is also designed for two collocated measurements at an arbitrary interior point, generating exponentially stable state estimates. The output feedback control law is formulated by composing the independently designed state-feedback controller with the observer, and the resulting dynamic feedback is shown to stabilize the trivial solution. Some numerical analysis on how the selection of these points affect the responses of the controller and observer are discussed, with simulations illustrating various choices of folding points and their effect on the stabilization in different performance indexes.**

***Index Terms*— backstepping, distributed parameter systems, multiple input, partial differential equations**

I. Introduction

PARABOLIC partial differential equations (PDEs) describe numerous physical processes, which include but are not limited to heat transfer, chemical reaction-diffusion processes, tumor angiogenesis [6], predator-prey Lotka-Volterra population models [12], opinion dynamics (of the Fischer-Kolmogorov-Petrovsky-Piskunov type equation [1]), free-electron plasma diffusion, and flows through porous media [19].

Previous results in boundary control for 1-D PDEs has been largely focused on unilateral boundary controllers, i.e. controllers acting on a single boundary. Results have been generated for a wide variety of parabolic PDE systems and objectives, beginning with the classical scalar 1-D PDE with homogeneous media results [13]. Other extensions to the parabolic PDE boundary control case introduce nonhomgeneous media (such as [16]), parallel interconnected parabolic PDE systems [22], series interconnected parabolic PDE systems [18], and output feedback extensions for coupled parabolic PDE [14]. Some work that is tangentially related is that of [23], [24], which investigates a problem of using an in-domain actuation to control a parabolic PDE.

The notion of bilateral boundary control is partially motivated by boundary control of balls in $\mathbb{R}^n$ [21], in which the controls actuate on the surface of the n-dimensional ball. The analogous case (in 1-D) is a controller actuating on the boundary of the 1-dimensional ball, i.e., the endpoints of an interval. Bilateral control has been studied in some contexts for both hyperbolic and parabolic PDE systems. [2] studies bilateral controllers achieving minimum-time convergence in coupled first-order hyperbolic systems via a Fredholm transformation technique, while [20] additionally studies bilateral control for diffusion-reaction equations, albeit with the limitatin of a symmetric Volterra transformation. [4] studies a nonlinear viscous Hamilton-Jacobi PDE, which likewise uses the symmetric Volterra transformation from [20].

Boundary observer design is of equal (and perhaps arguably more) importance when compared with the boundary controller design. Many results have been generated as a dual problem to the boundary controller case. In [15], a boundary observer design for parabolic PDEs is formulated, with measurements taken at a boundary (in both collocated and anticollocated cases). [3] studies a coupled parabolic PDE system with identical diffusion coefficients. [5] recovers a result for coupled parabolic PDEs with varying diffusion coefficients.

The main contribution of the paper are results for bilateral control of diffusion-reaction equations with spatially-varying reaction via the method of "folding," i.e. using an arbitrarily defined domain separation and transformation to design the boundary controllers. The idea of folding has been touched upon in the hyperbolic context [8], where the authors have explored a linearized Rijke tube model. The folding technique admits a design parameter (called the folding point) whose choice influences the control effort exerted by the boundary controllers. Additionally, a state-observer is designed to complement the state-feedback controller, in which collocated measurements in the interior are used to recover decoupled, classical backstepping observer designs. Finally, the output feedback is formulated by combining the state-feedback and state-estimation. Other related observer designs tackled via

The manuscript was submitted and received Nov. 5, 2020. R. Vazquez acknowledges funding from Spanish Ministerio de Ciencia, Innovación y Universidades under grant PGC2018-100680-B-C21

Stephen Chen was with the Department of Mechanical and Aerospace Engineering, University of California, San Diego, La Jolla, CA 92093-0411 USA (e-mail: stc007@ucsd.edu).

Rafael Vazquez is with the Departmento de Ingeniería Aeroespacial, Universidad de Sevilla, 41092 Sevilla, Spain (e-mail: rvazquez1@us.es).

Miroslav Krstic is with the Department of Mechanical and Aerospace Engineering, University of California, San Diego, La Jolla, CA 92093-0411 USA (e-mail: krstic@ucsd.edu).

the backsteppoing methodology include: [17], investigating observer designs where measurements are given as a weighted average (the state appearing underneath a bounded integral operator); [11], considering the combination of boundary measurements with a single interior measurement to achieve estimation convergence for semilinear parabolic problems.

The primary technical difficulty in the paper is compensating the folding-type boundary conditions, which arises due to the regularity property of the solutions. In hyperbolic PDE, this constitutes an imposition of continuity – a first-order compatibility condition. However, in parabolic PDE, one must treat second-order compatibility conditions existing at the same point, which will require additional correctional designs to compensate.

II. Preliminaries

A. Notation

In the paper, scalar values will be notated in lowercase, e.g. $f, g \in \mathbb{R}$. Vector and matrix values will be notated in uppercase, e.g. $A \in \mathbb{R}^2, B \in \mathbb{R}^{2\times 2}$. The components of vectors and matrices are denoted using lowercase with subscript. For vectors,

$$A = [a_i] = \begin{pmatrix} a_1 \\ a_2 \end{pmatrix}$$

while for matrices

$$B = [b_{ij}] = \begin{pmatrix} b_{11} & b_{12} \\ b_{21} & b_{22} \end{pmatrix}$$

Control input and output signals are further distinguished by calligraphic typefaces, e.g. $\mathcal{U}, \mathcal{V}, \mathcal{Y}$.

The partial operator is notated using the del-notation, i.e.

$$\partial_x f := \frac{\partial f}{\partial x}$$

$L^2(I_o)$ is defined as the the L^2 space on the interval I_o, equipped with the norm

$$||f||_{L^2(I_o)} = \left(\int_{I_o} f^2 \, d\mu \right)^{\frac{1}{2}}$$

We also consider the standard inner product (that induces the standard norm) for L^2:

$$\langle f, g \rangle_{L^2(I_o)} = \int_{I_o} f \cdot g \, d\mu$$

For compact notation, we will let $L^2(I_o)$ be represented merely as L^2, where the interval is implied by the function. The norm notation ($||\cdot||$) is used to notate the function norm over the vector 2-norm (notated with $|\cdot|_2$). If the norm is taken over a matrix function, then the induced 2-norm is implied, i.e. for vector-valued function f and matrix-valued function F:

$$||f||_{L^2} := \left(\int_{I_o} ||f||_2^2 \, d\mu \right)^{\frac{1}{2}}, \quad ||F||_{L^2} := \left(\int_{I_o} ||F||_{2,i}^2 \, d\mu \right)^{\frac{1}{2}}$$

Furthermore, if f is a function of the space-time tuple (x, t), the norm is assumed to be the norm in space (x) unless otherwise stated. The written x-dependence is dropped, i.e.

$$||f(x,t)||_{L^2} = ||f(t)||_{L^2} := \left(\int_{I_o} |f(t)|_2^2 \, d\mu \right)^{\frac{1}{2}}$$

We will introduce the notion of stability in the sense of a norm. Rigorously, this refers to the norm in which stability is derived. Per example, stability in the sense of L^2 refers to a stability estimate using L^2 norms:

$$||f(t)||_{L^2} \leq M \, ||f(t_0)||_{L^2}$$

Elements of a matrix A are denoted with lowercase a_{ij}, with the subscripts defining the i-th row and j-th column.

B. Model and problem formulation

We consider the following reaction-diffusion PDE for u on the domain $(-1, 1) \times [0, \infty)$:

$$\partial_t \bar{u}(y,t) = \varepsilon \partial_y^2 \bar{u}(y,t) + \nu(y) \partial_y \bar{u}(y,t) + \bar{\lambda}(y) \bar{u}(y,t) \quad (1)$$

$$\bar{u}(-1,t) = \bar{\mathcal{U}}_1(t) \quad (2)$$

$$\bar{u}(1,t) = \bar{\mathcal{U}}_2(t) \quad (3)$$

with the solution space $\bar{u} \in C(0, \infty; L^2(-1, 1))$. It is assumed that $\varepsilon > 0$, and $\nu, \bar{\lambda} \in C^1((-1, 1))$. The controllers operate at $x = 1$ and $x = -1$, and are denoted $\bar{\mathcal{U}}_1(t), \bar{\mathcal{U}}_2(t)$, respectively. We define the following transformation:

$$u(y,t) = \exp\left(\int_{-1}^{y} \frac{\nu(z)}{2\varepsilon} dz \right) \bar{u}(y,t) \quad (4)$$

We find the equivalent system

$$\partial_t u(y,t) = \varepsilon \partial_y^2 u(y,t) + \lambda(y) u(y,t) \quad (5)$$

$$u(-1,t) = \bar{\mathcal{U}}_1(t) =: \mathcal{U}_1(t) \quad (6)$$

$$u(1,t) = \exp\left(\int_{-1}^{1} \frac{\nu(z)}{2\varepsilon} dz \right) \bar{\mathcal{U}}_2(t) =: \mathcal{U}_2(t) \quad (7)$$

with the appropriate parameter definition:

$$\lambda(y) = \bar{\lambda}(y) - \frac{\nu'(y)}{2} \quad (8)$$

The transformation (4) removes the advection/convection term in (1). The attenuation/amplification of control effort in the controllers matches intuition – the controller upstream of the "average" convection requires less control effort, while the controller downstream requires more control effort (average, as the sign of ν can vary across the domain).

The output, denoted $\mathcal{Y}$, is formulated as

$$\mathcal{Y}(t) = \begin{pmatrix} u(\hat{y}_0, t) \\ \partial_y u(\hat{y}_0, t) \end{pmatrix} \quad (9)$$

where $\hat{y}_0$ is a point that exists inside the domain of the evolution equation (5) (i.e., not occuring at a boundary). The output consists of a *collocated* point measurement of state and flux.

The output feedback can be summarized succintly in two subproblems:

1) Bilateral state-feedback control design

2) Collocated in-domain measurement state-observer design Finally, by showing a separation principle holds between the two subproblems, one can synthesize a certainty-equivalence output-feedback control design by combining the two. These steps will be designed and analyzed in the following sections via the utilization of a *folding* transformation in conjunction with continuum backstepping designs.

III. Output-feedback control design

A. Model transformation for control via folding

The folding approach entails selecting a point $y_0 \in (-1, 1)$ in which the scalar parabolic PDE system u is "folded" into a 2×2 coupled parabolic system. A special case $y_0 = 0$ (dividing into a symmetric problem) recovers the result of [20]. We define the the folding spatial transformations as

$$x = (y_0 - y)/(1 + y_0) \qquad y \in (-1, y_0) \tag{10}$$
$$x = (y - y_0)/(1 - y_0) \qquad y \in (y_0, 1) \tag{11}$$

admits the following states:

$$U(x,t) := \begin{pmatrix} u_1(x,t) \\ u_2(x,t) \end{pmatrix} = \begin{pmatrix} u(y_0 - (1+y_0)x, t) \\ u(y_0 + (1-y_0)x, t) \end{pmatrix} \tag{12}$$

One technical note to mention is that in this formulation, we consider the notion of a solution $U \in C(0,\infty; L^2(0,1))^2$, which is almost equivalent to u and therefore $\bar{u}$ in an L^2-sense, via the aforementioned spatial transformation.

whose dynamics are governed by the following system:

$$\partial_t U(x,t) = E\partial_x^2 U(x,t) + \Lambda(x)U(x,t) \tag{13}$$
$$\alpha\partial_x U(0,t) = -\beta U(0,t) \tag{14}$$
$$U(1,t) = \mathcal{U}(t) \tag{15}$$

with the parameters given by:

$$\begin{aligned} E &:= \text{diag}(\varepsilon_1, \varepsilon_2) \\ &:= \text{diag}\left(\frac{\varepsilon}{(1+y_0)^2}, \frac{\varepsilon}{(1-y_0)^2}\right) \end{aligned} \tag{16}$$
$$\begin{aligned} \Lambda(x) &:= \text{diag}(\lambda_1(x), \lambda_2(x)) \\ &:= \text{diag}(\lambda(y_0 - (1+y_0)x), \lambda(y_0 + (1-y_0)x)) \end{aligned} \tag{17}$$
$$\alpha := \begin{pmatrix} 1 & a \\ 0 & 0 \end{pmatrix} \tag{18}$$
$$\beta := \begin{pmatrix} 0 & 0 \\ 1 & -1 \end{pmatrix} \tag{19}$$
$$a := (1 + y_0)/(1 - y_0) \tag{20}$$

The control inputs are collected into the vector $\mathcal{U}(t) := \begin{pmatrix} \mathcal{U}_1(t) & \mathcal{U}_2(t) \end{pmatrix}^T$.

The boundary conditions at $x = 0$ are curious. While they may initially appear to be encapsulated as Robin boundary conditions in (14), they are actually compatibility conditions that arise from imposing the following conditions on continuity in the solution at the folding point:

$$\lim_{y \to y_0^-} u(y,t) = \lim_{y \to y_0^+} u(y,t) \tag{21}$$
$$\lim_{y \to y_0^-} \partial_y u(y,t) = \lim_{y \to y_0^+} \partial_y u(y,t) \tag{22}$$

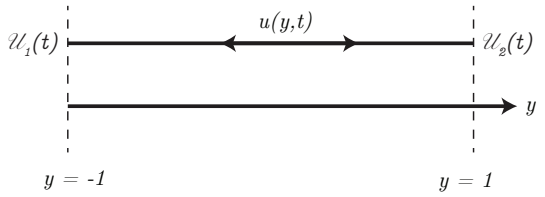

Fig. 1. System schematic of diffusion-reaction equation with two boundary inputs. The control folding point y_0 and the measurement location $\hat{y_0}$ can be arbitrarily chosen on the interior, independent of one another.

With some mild assumptions on the initial and compatiblity conditions, the target parabolic equations (13)-(15) are relatively well-behaved and have regular solutions. As we show in Section IV, the backstepping transformations developed will have certain regularity properties, which can relate (13)-(15) with (1)-(3).

Conditions (21)-(22) arise in the folded state as a pair of boundary conditions at $x = 0$:

$$u_1(0,t) = u_2(0,t) \tag{23}$$
$$\partial_x u_1(0,t) = -a\partial_x u_2(0,t) \tag{24}$$

Analogous conditions have been considered in some previous parabolic backstepping work in [18], albeit in a different context.

Assumption 1. *The folding point y_0 is restricted to the half domain $(-1, 0]$ without loss of generality. The case $y_0 \in [0, 1)$ can be recovered by using a change in spatial variables $\hat{y} = -y$ and performing the same folding technique. By choosing y_0 in this manner, we impose an ordering $\varepsilon_1 > \varepsilon_2$.*

B. State-feedback design

The backstepping state-feedback control design is accomplished with two consecutive backstepping transformations. The first transformation is a 2×2 Volterra integral transformation of the second kind:

$$W(x,t) = U(x,t) - \int_0^x K(x,y)U(y,t)dy \tag{25}$$

where $K(x,y) \in C^2(\mathcal{T})$ is a 2×2 matrix of kernel elements (k_{ij}), with $\mathcal{T} := \{(x,y) \in \mathbb{R}^2 | 0 \le y \le x \le 1\}$, and $W(x,t) := \begin{pmatrix} w_1(x,t) & w_2(x,t) \end{pmatrix}^T$. The inverse transformation is analogous:

$$U(x,t) = W(x,t) - \int_0^x \bar{K}(x,y)W(y,t)dy \tag{26}$$

The corresponding target system for (25) is chosen to be

$$\partial_t W(x,t) = E\partial_x^2 W(x,t) - CW(x,t) + G[K](x)W(x,t) \tag{27}$$
$$\alpha\partial_x W(0,t) = -\beta W(0,t) \tag{28}$$
$$W(1,t) = \mathcal{V}(t) \tag{29}$$

where $\mathcal{V}(t) = \begin{pmatrix} 0 & \nu_2(t) \end{pmatrix}^T$ is an auxiliary control which is designed later in the paper. The controller $\mathcal{U}(t)$ can be

expressed in an affine relationship to $\mathcal{V}(t)$ by evaluating (25) for $x = 1$:

$$\mathcal{U}(t) := \mathcal{V}(t) + \int_0^1 K(1,y)U(y,t)dy \tag{30}$$

The matrix C can be arbitrarily chosen such that $C \succ 0$, but for simplicity of analysis, we select a diagonal matrix $C = \text{diag}(c_1, c_2)$ with $c_1, c_2 > 0$. The matrix-valued operator $G[\cdot](x)$ acting on K is given by

$$G[K](x) = \begin{pmatrix} 0 & 0 \\ (\varepsilon_2 - \varepsilon_1)\partial_y k_{21}(x,x) & 0 \end{pmatrix} =: \begin{pmatrix} 0 & 0 \\ g[k_{21}](x) & 0 \end{pmatrix} \tag{31}$$

The second transformation is designed to admit an expression for the auxiliary controller $\mathcal{V}(t) = \begin{pmatrix} 0 & \nu_2(t) \end{pmatrix}^T$. The goal of $\nu_2(t)$ is to remove the potentially destabilizing effect of the coupling term $G[K](x)$. The second set of transformations is:

$$\omega_1(x,t) = w_1(x,t) \tag{32}$$

$$\omega_2(x,t) = w_2(x,t) - \int_0^x \begin{pmatrix} q(x,y) & p(x-y) \end{pmatrix} W(y,t)dy - \int_x^1 \begin{pmatrix} r(x,y) & 0 \end{pmatrix} W(y,t)dy \tag{33}$$

Let $\Omega(x,t) := \begin{pmatrix} \omega_1(x,t) & \omega_2(x,t) \end{pmatrix}^T$. The inverse transformations are given by

$$w_1(x,t) = \omega_1(x,t) \tag{34}$$

$$w_2(x,t) = \omega_2(x,t) - \int_0^x \begin{pmatrix} \bar{q}(x,y) & \bar{p}(x-y) \end{pmatrix} \Omega(y,t)dy - \int_x^1 \begin{pmatrix} \bar{r}(x,y) & 0 \end{pmatrix} \Omega(y,t)dy \tag{35}$$

We impose the following target system dynamics:

$$\partial_t \Omega(x,t) = E\partial_x^2 \Omega(x,t) - C\Omega(x,t) \tag{36}$$

$$\alpha \partial_x \Omega(0,t) = -\beta \Omega(0,t) \tag{37}$$

$$\Omega(1,t) = 0 \tag{38}$$

Noting that $G[K](x)$ is parametrized by the difference in diffusion coefficients $\varepsilon_1 - \varepsilon_2$, one can interpret (33) to be the *correction* factor to the first transformation in presence of selecting a non-trivial folding point. Indeed, when the folding point is chosen to be the midpoint, $G[K](x) \equiv 0$ (and therefore (33) becomes an identity transformation). This necessity for correction factors is to compensate for the behavior unique to bilateral control design in parabolic PDE, and is not observed in the results featuring bilateral control design of hyperbolic PDE systems [2].

The transformation (33) features two major components – a Volterra integral operator in w_2 characterized by kernel p, a Volterra integral operator in w_1 characterized by kernel q, and a *forwarding* type of transformation in w_1 characterized by kernel r. The kernels p, q are defined on the domain $\mathcal{T}$, while r is defined on the domain $\mathcal{T}_u := \{(x,y) \in \mathbb{R}^2 | 0 \le x \le y \le 1\}$.

Lemma 2. *The trivial solution $\Omega \equiv 0$ of the target system* (36)-(38) *is exponentially stable in the sense of the L^2 norm. That is,*

$$||\Omega(\cdot,t)||_{L^2} \le \Pi \exp(-\gamma t) ||\Omega(\cdot,0)||_{L^2} \tag{39}$$

where the constants Π, γ are given by

$$\Pi = a^{-\frac{3}{2}} \tag{40}$$

$$\gamma = \min\{a^3 c_1, c_2\} + \frac{\varepsilon_2}{4} \tag{41}$$

We omit the proof for space, but the result follows in a straightforward manner using the following Lyapunov function v:

$$v(t) := \int_0^1 \Omega(x,t)^T A \Omega(x,t)dx \tag{42}$$

where $A = \text{diag}(a^3, 1)$.

With Lemma 2, we are equipped to establish state feedback result.

Theorem 3. *Let the initial data $\bar{u}(\cdot,0) \in H^1(-1,1)$ satisfy the zero-th order compatibility conditions*

$$\begin{pmatrix} \bar{\mathcal{U}}_1(0) \\ \bar{\mathcal{U}}_2(0) \end{pmatrix} = \int_{-1}^1 \begin{pmatrix} f_1(y) \\ f_2(y) \end{pmatrix} \bar{u}(y,0)dy \tag{43}$$

and let the pair of feedback controllers $\bar{\mathcal{U}}_1, \bar{\mathcal{U}}_2$ be defined as

$$\begin{pmatrix} \bar{\mathcal{U}}_1(t) \\ \bar{\mathcal{U}}_2(t) \end{pmatrix} = \int_{-1}^1 \begin{pmatrix} f_1(y) \\ f_2(y) \end{pmatrix} \bar{u}(y,t)dy \tag{44}$$

with feedback gains f_1, f_2

$$f_1(y) = \begin{cases} (1+y_0)^{-1} k_{11}\left(1, \frac{y_0 - y}{1+y_0}\right) & y \le y_0 \\ (1-y_0)^{-1} k_{12}\left(1, \frac{y - y_0}{1-y_0}\right) & y > y_0 \end{cases} \tag{45}$$

$$f_2(y) = \begin{cases} (1+y_0)^{-1} h_1\left(\frac{y_0 - y}{1+y_0}\right) & y \le y_0 \\ (1-y_0)^{-1} h_2\left(\frac{y - y_0}{1-y_0}\right) & y > y_0 \end{cases} \tag{46}$$

$$h_1(y) = k_{21}(1,y) + q(1,y) - \int_y^1 \left[p(1-z)k_{21}(z,y) + q(1,z)k_{11}(z,y)\right]dz \tag{47}$$

$$h_2(y) = k_{22}(1,y) + p(1-y) - \int_y^1 \left[p(1-z)k_{22}(z,y) + q(1,z)k_{12}(z,y)\right]dz \tag{48}$$

where $k_{ij} \in C^2(\mathcal{T})$ and $p, q \in C^1(\mathcal{T})$ are solutions to the kernel equations (96),(110),(111) *respectively (with associated boundary conditions). Then there exists a unique solution $\bar{u} \in C(R^+, L(-1,1))$ under feedback* (44)*. Additionally, the trivial solution of the system* (1)-(3) *is exponentially stable in the sense of the L^2 norm, that is, there exists a constant $\bar{\pi}$ such that*

$$||\bar{u}(\cdot,t)||_{L^2} \le \bar{\pi} \exp(-\gamma t) ||\bar{u}(\cdot,0)||_{L^2} \tag{49}$$

Proof. The well-posedness follows from §7.1.3, Thm. 5.(i) in [10] under the zero-th order compatibility conditions.

The feedback controllers (44) are derived via evaluating transforms (25),(33) at the boundary $x = 1$. From (33):

$$W(1,t) = \mathcal{V}(t) = \begin{pmatrix} 0 \\ \nu_2(t) \end{pmatrix} = \begin{pmatrix} 0 \\ \int_0^1 \begin{pmatrix} q(1,y) & p(1-y) \end{pmatrix} W(y,t)dy \end{pmatrix} \tag{50}$$

From (25),(30):

$$\mathcal{U}(t) = \int_0^1 K(1,y)U(y,t)dy + \mathcal{V}(t) \tag{51}$$

Or componentwise,

$$\mathcal{U}_1(t) = \int_0^1 \begin{pmatrix} k_{11}(1,y) & k_{12}(1,y) \end{pmatrix} U(y,t)dy \tag{52}$$

$$\begin{aligned}\mathcal{U}_2(t) = &\int_0^1 \begin{pmatrix} k_{21}(1,y) & k_{22}(1,y) \end{pmatrix} U(y,t)dy \\ &+ \int_0^1 \begin{pmatrix} q(1,y) & p(1-y) \end{pmatrix} U(y,t)dy \\ &- \int_0^1 \int_0^y K(y,z)U(z,t)dzdy\end{aligned} \tag{53}$$

By exchanging the order of integrals in the nested integrals, and applying the inverse folding transformations (12), the controllers (44) can be recovered.

The proof of the bound (49) relies on the well-posedness of the kernel PDEs, studied in Section IV. Specifically, Lemmas 8,9,10 state that continuous solutions exist and are unique. By Morrey's inequality (5.6.2 Theorem 4 in [10]), the continuous embedding $C^1(\mathcal{T}) \hookrightarrow L^2(\mathcal{T})$ holds, and therefore $C^1(\mathcal{T})$ functions possess a bounded $L^2(\mathcal{T})$ norm. The boundedness (in $L^2(\mathcal{T})$) of the kernels K, p, q, r (and their inverses $\bar{K}, \bar{p}, \bar{q}, \bar{r}$) are required, but can be shown from their continuity properties on the compact sets $\mathcal{T}, \mathcal{T}_{\mathsf{u}}$.

From (33), (35), one can derive the following equivalence:

$$m_1^{-1} ||W(\cdot,t)||_{L^2}^2 \leq ||\Omega(\cdot,t)||_{L^2}^2 \leq \bar{m}_1 ||W(\cdot,t)||_{L^2}^2 \tag{54}$$

where the coefficient m_1 depends on kernels p, q, r, and is given by

$$m_1 = (1 - ||q||_{L^2} - ||p||_{L^2} - ||r||_{L^2})^2 \tag{55}$$

and $\bar{m}_1$ is analogous with inverse kernels $\bar{p}, \bar{q}, \bar{r}$. Similarly, from (25),(26), the following equivalence can be derived:

$$\bar{m}_2^{-1} ||U(\cdot,t)||_{L^2}^2 \leq ||W(\cdot,t)||_{L^2}^2 \leq m_2 ||U(\cdot,t)||_{L^2}^2 \tag{56}$$

with

$$m_2 = (1 - ||K||_{L^2})^2 \tag{57}$$

and $\bar{m}_2$ analogous with inverse kernel $\bar{K}$. Then, applying (54),(56) to the bound (39) in Lemma 2, one can arrive at (49), with

$$\bar{\pi} = \left(\sqrt{m_1 \bar{m}_1 m_2 \bar{m}_2}\right) \Pi \tag{58}$$

□

C. Model transformation for estimation via folding

We begin by emphasizing that the sensor location $\hat{y}_0$ is *independent* of the chosen control folding point y_0. Similar to the state-feedback control design, we first apply a folding transformation (this time, about $\hat{y}_0$), and recover a coupled parabolic system. The transformation

$$\hat{x} = (\hat{y}_0 - y)/(1 + \hat{y}_0) \qquad y \in (-1, \hat{y}_0) \tag{59}$$

$$\hat{x} = (y - \hat{y}_0)/(1 - \hat{y}_0) \qquad y \in (\hat{y}_0, 1) \tag{60}$$

will admit the following folded states:

$$\check{U}(\hat{x},t) := \begin{pmatrix} \check{u}_1(\hat{x},t) \\ \check{u}_2(\hat{x},t) \end{pmatrix} = \begin{pmatrix} u(\hat{y}_0 - (1+\hat{y}_0)\hat{x}, t) \\ u(\hat{y}_0 + (1-\hat{y}_0)\hat{x}, t) \end{pmatrix} \tag{61}$$

The evolution of $\check{U}(x,t)$ governed by the following dynamics:

$$\partial_t \check{U}(x,t) = \check{E}\partial_x^2 \check{U}(x,t) + \check{\Lambda}(x)\check{U}(x,t) \tag{62}$$

$$\check{\alpha}\partial_x \check{U}(0,t) = -\beta \check{U}(0,t) \tag{63}$$

$$\check{U}(1,t) = \mathcal{U}(t) \tag{64}$$

The hat notation on $\hat{x}$ has been dropped for simplicity and the spatial domains are defined within the context of the equation in which it arises. The parameter matrices are then as follows:

$$\begin{aligned}\check{E} &:= \text{diag}(\check{\varepsilon}_1, \check{\varepsilon}_2) \\ &:= \text{diag}\left(\frac{\varepsilon}{(1+\hat{y}_0)^2}, \frac{\varepsilon}{(1-\hat{y}_0)^2}\right)\end{aligned} \tag{65}$$

$$\begin{aligned}\check{\Lambda}(x) &:= \text{diag}(\check{\lambda}_1(x), \check{\lambda}_2(x)) \\ &:= \text{diag}(\lambda(\hat{y}_0 - (1+\hat{y}_0)x), \lambda(\hat{y}_0 + (1-\hat{y}_0)x))\end{aligned} \tag{66}$$

$$\check{\alpha} := \begin{pmatrix} 1 & \check{a} \\ 0 & 0 \end{pmatrix} \tag{67}$$

$$\check{a} := (1+\hat{y}_0)/(1-\hat{y}_0) \tag{68}$$

Certainly, if $\hat{y}_0 = y_0$, then the observation and control folded models are identical.

D. Backstepping state observer design

Note that the sensor values in the folded coordinates can be expressed in the following manner:

$$\begin{pmatrix} u(\hat{y}_0, t) \\ \partial_y u(\hat{y}_0, t) \end{pmatrix} = \begin{pmatrix} u_1(0,t) \\ -(1+y_0)^{-1}\partial_x u_1(0,t) \end{pmatrix} \tag{69}$$

$$= \begin{pmatrix} u_2(0,t) \\ (1-y_0)^{-1}\partial_x u_2(0,t) \end{pmatrix} \tag{70}$$

With the two sensor values collocated at a single point, the design of the state observer can be decoupled into two near-identical classical backstepping observer subproblems. Specifically, we choose the following observer structure (indexed by $i \in \{1,2\}$):

$$\begin{aligned}\partial_t \hat{u}_i = &\check{\varepsilon}_i \partial_x^2 \hat{u}_i(x,t) + \check{\lambda}_i(x)\hat{u}_i(x,t) \\ &+ \phi_i(x)\left(\partial_x u_i(0,t) - \partial_x \hat{u}_i(0,t)\right)\end{aligned} \tag{71}$$

$$\hat{u}_i(0,t) = u(0,t) \tag{72}$$

$$\hat{u}_i(1,t) = \mathcal{U}_i(t) \tag{73}$$

where the functions $\phi_i \in L^2(0,1)$ are corrective observer injection gains to be determined.

We define the error systems of the observers as $\tilde{u}_i(x,t) := u_i(x,t) - \hat{u}_i(x,t)$. They are governed by

$$\begin{aligned}\partial_t \tilde{u}_i = &\check{\varepsilon}_i \partial_x^2 \tilde{u}_i(x,t) + \check{\lambda}_i(x)\tilde{u}_i(x,t) \\ &- \phi_i(x)\partial_x \tilde{u}_i(0,t)\end{aligned} \tag{74}$$

$$\tilde{u}_i(0,t) = 0 \tag{75}$$

$$\tilde{u}_i(1,t) = 0 \tag{76}$$

We can then design the $\phi_i(x)$ independently to stabilize trivial solutions $\tilde{u}_i(x,t) \equiv 0$ of the error systems $\tilde{u}_i$. We employ the following pair of backstepping transformations

$$\tilde{w}_i(x,t) = \tilde{u}_i(x,t) - \int_0^x \Phi_i(x,y)\tilde{u}_i(y,t)dy \tag{77}$$

with the following target systems:

$$\partial_t \tilde{w}_i(x,t) = \check{\varepsilon}_i \partial_x^2 \tilde{w}_i(x,t) - \check{c}_i \tilde{w}_i(x,t) \tag{78}$$
$$\tilde{w}_i(0,t) = 0 \tag{79}$$
$$\tilde{w}_i(1,t) = 0 \tag{80}$$

The inverse transformations are postulated to be

$$\tilde{u}_i(x,t) = \tilde{w}_i(x,t) - \int_0^x \bar{\Phi}_i(x,y)\tilde{w}_i(y,t)dy \tag{81}$$

where $\bar{\Phi}_i(x,y)$ will satisfy similar kernel equations to Φ.

Lemma 4. *For the choice of coefficients $\check{c}_i > 0, i \in \{1,2\}$, the trivial solutions $(\tilde{w}_i, \tilde{v}_i) \equiv 0$ of the observer error target systems* (78)-(80) *are exponentially stable in the L^2 sense, that is, there exist coefficients $\check{\pi}_i, \check{\gamma}_i > 0$ such that for $i \in \{1,2\}$,*

$$||\tilde{w}_i(\cdot,t)||_{L^2} \leq \check{\pi}_i \exp(-\check{\gamma}_i t)\, ||\tilde{w}_i(\cdot,0)||_{L^2} \tag{82}$$

The proof of Lemma 4 can be found in [15].

Theorem 5. *Consider the original system* (5)-(7) *and the auxiliary observer system defined in* (71)-(73) *with measurements $u(0,t), \partial_y u(0,t)$. Define the state estimate*

$$\hat{u}(y,t) := \begin{cases} \hat{u}_1\left(\frac{\hat{y}_0 - y}{1+\hat{y}_0}\right) & y \leq \hat{y}_0 \\ \hat{u}_2\left(\frac{y-\hat{y}_0}{1-\hat{y}_0}\right) & y > \hat{y}_0 \end{cases} \tag{83}$$

and

$$\hat{\tilde{u}}(y,t) := \exp\left(-\int_{-1}^{y} \frac{\nu(z)}{2\varepsilon} dz\right) \hat{u}(y,t) \tag{84}$$

Then $\hat{\tilde{u}}(y,t) \to \bar{u}(y,t)$ exponentially fast in the sense of the L^2 norm, i.e. there exist coefficients $\check{\bar{\pi}}, \check{\gamma}_{min} > 0$ such that

$$\left|\left|\bar{u}(\cdot,t) - \hat{\tilde{u}}(\cdot,t)\right|\right|_{L^2} \leq \check{\bar{\pi}} \exp(-\check{\gamma}_{min} t) \left|\left|\bar{u}(\cdot,0) - \hat{\tilde{u}}(\cdot,0)\right|\right|_{L^2} \tag{85}$$

We omit the proof for space, but note that it follows directly from Lemmas 4, 7. By applying successive inverse transformations, the bound (85) can be recovered.

E. Output-feedback controller

The output feedback controller proposed is the composition of the state observer with the state feedback. We state the main result below:

Theorem 6 (Separation principle)**.** *Consider the original system* (5)-(7) *and the auxiliary observer system defined in* (71)-(73) *with measurements $u(0,t), \partial_y u(0,t)$. With the state estimate* (83)*, the feedback controller pair $\bar{\mathcal{U}}_1(t), \bar{\mathcal{U}}_2(t)$:*

$$\begin{pmatrix} \bar{\mathcal{U}}_1(t) \\ \bar{\mathcal{U}}_2(t) \end{pmatrix} = \int_{-1}^{1} \begin{pmatrix} f_1(y) \\ f_2(y) \end{pmatrix} \hat{u}(y,t)dy \tag{86}$$

with the gains f_1, f_2 defined in (45),(46) *will stabilize $(\bar{u}, \hat{\tilde{u}}) \equiv 0$ exponentially in the L^2 sense – that is, there exist constants $\bar{\bar{\pi}}, \bar{\bar{\gamma}} > 0$ such that*

$$\left|\left|(\bar{u}, \hat{\tilde{u}})(\cdot,t)\right|\right|_{L^2} \leq \bar{\bar{\pi}} \exp(\bar{\bar{\gamma}} t) \left|\left|(\bar{u}, \hat{\tilde{u}})(\cdot,0)\right|\right|_{L^2} \tag{87}$$

Proof. The output feedback control law (86) is rewritten in the $(\bar{u}, \tilde{\tilde{u}})$ coordinates (recalling that $\tilde{\tilde{u}} := \bar{u} - \hat{\tilde{u}}$):

$$\begin{pmatrix} \bar{\mathcal{U}}_1(t) \\ \bar{\mathcal{U}}_2(t) \end{pmatrix} = \int_{-1}^{1} \begin{pmatrix} f_1(y) \\ f_2(y) \end{pmatrix} \bar{u}(y,t)dy + \int_{-1}^{1} \begin{pmatrix} f_1(y) \\ f_2(y) \end{pmatrix} \tilde{\tilde{u}}(y,t)dy \tag{88}$$

Applying the transformations (25),(33) will yield the same target system (36),(37), with the modified boundary condition

$$\Omega(1,t) = \int_{-1}^{1} \begin{pmatrix} f_1(y) \\ f_2(y) \end{pmatrix} \tilde{\tilde{u}}(y,t)dy \tag{89}$$

Applying the Cauchy-Schwarz inequality and the bound from Theorem 5, we can bound this boundary condition in the following manner:

$$||\Omega(1,t)||_2 \leq \check{\bar{\pi}} \left|\left| \begin{pmatrix} f_1(y) \\ f_2(y) \end{pmatrix} \right|\right|_{L^2} ||\tilde{\tilde{u}}(\cdot,0)||_{L^2} \times \exp(-\check{\gamma}_{\min} t) \tag{90}$$

Following the proof of Lemma 2 and Theorem 3, one can arrive at the following inequality on the L^2 norm of the system state:

$$||\bar{u}(\cdot,t)||_{L^2} \leq \bar{\pi} \exp(-\bar{\gamma} t)\, ||\bar{u}(\cdot,0)||_{L^2} + \hat{\bar{\pi}} \exp\left(-\min\{\bar{\gamma}, \check{\gamma}\} t\right) ||\tilde{\tilde{u}}(\cdot,0)||_{L^2} \tag{91}$$

where

$$\hat{\bar{\pi}} = (1 + ||p||_{L^2} + ||q||_{L^2})(1 + ||K||_{L^2}) \times \left|\left| \begin{pmatrix} f_1 \\ f_2 \end{pmatrix} \right|\right|_{L^2} \frac{\check{\bar{\pi}}}{\sqrt{2|\bar{\gamma} - \check{\gamma}_{\max}|}} \tag{92}$$

Taking the root sum square of (85) and (91), one can arrive at an exponential stability result for $(\bar{u}, \tilde{\tilde{u}})$:

$$||(\bar{u}, \tilde{\tilde{u}})(\cdot,t)||_{L^2} \leq \tilde{\bar{\pi}} \exp\left(-\bar{\bar{\gamma}} t\right) ||(\bar{u}, \tilde{\tilde{u}})(\cdot,0)||_{L^2} \tag{93}$$

where

$$\tilde{\bar{\pi}} = \max\{\bar{\pi}, \hat{\bar{\pi}} + \check{\bar{\pi}}\} \tag{94}$$
$$\bar{\bar{\gamma}} = \min\{\bar{\gamma}, \check{\gamma}\} \tag{95}$$

Finally, transforming back into the $(\bar{u}, \hat{u})$ coordinates, (87) can be recovered, with $\bar{\bar{\pi}} = 4\tilde{\bar{\pi}}$. □

F. Kernel PDE derivations

1) K-PDE derivation: Imposing the conditions (13), (14), (25), (27)-(29) admits the following companion gain kernel PDE system for $K(x,y)$:

$$E\partial_x^2 K(x,y) - \partial_y^2 K(x,y)E = K(x,y)\Lambda(y) + CK(x,y) - G[K](x)K(x,y) \tag{96}$$

$$\partial_y K(x,x)E + E\partial_x K(x,x) = -E\frac{d}{dx}K(x,x) - \Lambda(x) - C + G[K](x) \quad (97)$$

$$EK(x,x) - K(x,x)E = 0 \quad (98)$$

$$K(x,0)E\partial_x U(0,t) = \partial_y K(x,0)EU(0,t) \quad (99)$$

It is clear to see that by imposing (98), the definition for $G[K](x)$ can be recovered from (97). Upon first inspection, the resulting kernel PDE is very similar to those found in [22], [9]. However, one may see that (99) is different, and in fact quite new in backstepping designs. (99) arises due to the folding boundary condition (14). Surprisingly enough, if one analyzes (99) componentwise and employs (14), "anti-folding" conditions on K can be recovered, which preserve continuity in the spatial derivative of the state (as opposed to folding conditions preserving continuity in the state). The folding conditions that arise from (99) are:

$$a\varepsilon_1 k_{11}(x,0) - \varepsilon_2 k_{12}(x,0) = 0 \quad (100)$$

$$\varepsilon_1\partial_y k_{11}(x,0) + \varepsilon_2\partial_y k_{12}(x,0) = 0 \quad (101)$$

$$a\varepsilon_1 k_{21}(x,0) - \varepsilon_2 k_{22}(x,0) = 0 \quad (102)$$

$$\varepsilon_1\partial_y k_{21}(x,0) + \varepsilon_2\partial_y k_{22}(x,0) = 0 \quad (103)$$

or, more compactly written,

$$\tilde{\alpha}K(x,0) = \tilde{\beta}\partial_y K(x,0) \quad (104)$$

where

$$\tilde{\alpha} := \begin{pmatrix} a & -1 \\ 0 & 0 \end{pmatrix}, \quad \tilde{\beta} := \begin{pmatrix} 0 & 0 \\ 1 & 1 \end{pmatrix}. \quad (105)$$

The kernel equations for the inverse kernels $\bar{K}$ are similar to those of K, and are derived in an analogous manner:

$$E\partial_x^2\bar{K}(x,y) - \partial_y^2\bar{K}(x,y)E = -\bar{K}(x,y)(C - G[\bar{K}](y)) - \Lambda(x)\bar{K}(x,y) \quad (106)$$

$$\partial_y\bar{K}(x,x)E + E\partial_x\bar{K}(x,x) = -E\frac{d}{dx}\bar{K}(x,x) + \Lambda(x) + C - G[\bar{K}](x) \quad (107)$$

$$E\bar{K}(x,x) - \bar{K}(x,x)E = 0 \quad (108)$$

$$\bar{K}(x,0)E\partial_x W(0) = \partial_y\bar{K}(x,0)EW(0) \quad (109)$$

Of importance to note is that the inverse $\bar{K}$ kernel possess the same structure as the forward kernel K, and thus, the well-posedness of the inverse $\bar{K}$ naturally follows from the well-posedness of K.

2) (p, q, r)-PDE derivation: The transformation (33) with the conditions (27)-(29),(36)-(38) imposed will admit the following definition for p and kernel PDEs for q, r:

$$p(x) = a^{-1}q(x,0) \quad (110)$$

$$\varepsilon_2\partial_x^2 q(x,y) - \varepsilon_1\partial_y^2 q(x,y) = (c_2 - c_1)q(x,y) + g[k_{21}](y)p(x-y) \quad (111)$$

$$\varepsilon_2\partial_x^2 r(x,y) - \varepsilon_1\partial_y^2 r(x,y) = (c_2 - c_1)r(x,y) \quad (112)$$

subject to the following boundary conditions:

$$\partial_y q(x,x) = \partial_y r(x,x) + \frac{g[k_{21}](x)}{\varepsilon_2 - \varepsilon_1} \quad (113)$$

$$r(x,x) = q(x,x) \quad (114)$$

$$\partial_y q(x,0) = a^2 p'(x) = a\partial_x q(x,0) \quad (115)$$

$$r(x,1) = 0 \quad (116)$$

In addition, two initial conditions on r can be found from enforcing (28) on (33):

$$r(0,y) = 0 \quad (117)$$

$$\partial_x r(0,y) = \mathbf{1}_{\{y=0\}}(y)\frac{g[k_{21}](0)}{\varepsilon_2 - \varepsilon_1} \quad (118)$$

where $\mathbf{1}_{\{y=0\}}(y)$ is the indicator function equal to 1 on the set $\{y = 0\}$ and 0 otherwise. This is quite unusual when compared to standard backstepping techniques, but is necessary to resolve the condition (113),(114) at $x = y = 0$. Despite having this unusual initial condition, the target system and gain kernels are unaffected as $\partial_x r(0,y)$ only appears underneath an integration operation. The kernel equations for the inverse kernels $\bar{p}, \bar{q}, \bar{r}$ are similar to those of p, q respectively:

$$\bar{p}(x) = a^{-1}\bar{q}(x,0) \quad (119)$$

$$\varepsilon_2\partial_x^2\bar{q}(x,y) - \varepsilon_1\partial_y^2\bar{q}(x,y) = (c_1 - c_2)\bar{q}(x,y) - g[k_{21}](x)\bar{p}(x-y) \quad (120)$$

$$\varepsilon_2\partial_x^2\bar{r}(x,y) - \varepsilon_1\partial_y^2\bar{r}(x,y) = (c_2 - c_1)\bar{r}(x,y) \quad (121)$$

with boundary conditions

$$\partial_y\bar{q}(x,x) = \partial_y\bar{r}(x,x) + \frac{g[k_{21}](x)}{\varepsilon_1 - \varepsilon_2} \quad (122)$$

$$\bar{r}(x,x) = \bar{q}(x,x) \quad (123)$$

$$\partial_y\bar{q}(x,0) = -a^2\bar{p}'(x) = -a\partial_x\bar{q}(x,0) \quad (124)$$

$$\bar{r}(x,1) = 0 \quad (125)$$

As in the forward transformation, initial conditions on $\bar{r}$ can be found:

$$\bar{r}(0,y) = 0 \quad (126)$$

$$\partial_x\bar{r}(0,y) = \mathbf{1}_{\{y=0\}}(y)\frac{g[k_{21}](0)}{\varepsilon_1 - \varepsilon_2} \quad (127)$$

Similar to the first transformation, the inverse $\bar{p}, \bar{q}, \bar{r}$ kernels possess the same structure as the forward kernel p, q, r, and well-posedness of the inverse kernels $\bar{p}, \bar{q}, \bar{r}$ naturally follows the well-posedness of the forward kernels p, q, r.

An interpretation of the (p, q, r) coupled kernel is that of a hyperbolic PDE (q, r) defined on the square $\mathcal{T} \cup \mathcal{T}_{\mathrm{u}}$, subject to non-local coupling and memory phenomena via p. Transmission conditions between q, r exist at the interface $y = x$, where operator $g[k_{21}](x)$ acts as a point forcing through the interface. This interpretation will motivate the well-posedness study of (p, q, r). A point of interest to be raised is on the postulated continuity of the solutions. From (114), continuity is imposed between q, r, however, due to (113), the partial derivatives will not exhibit the same property. One may expect piecewise differentiability, in which the derivative loses continuity at the interface $y = x$.

3) $\Phi_{1,2}$-PDE derivation: The companion gain kernel PDEs for Φ_i can be found from imposing conditions arising from (62)-(64), (78)-(80), and the transformation (77).

$$\partial_x^2\Phi_i(x,y) - \partial_y^2\Phi_i(x,y) = -\frac{\lambda_i(x) + c_i}{\varepsilon_i}\Phi_i(x,y) \quad (128)$$

$$\Phi_i(1,y) = 0 \tag{129}$$

$$\Phi_i(x,x) = \int_x^1 \frac{\lambda_i(y)+c_i}{2\varepsilon_i} dy \tag{130}$$

In addition, one additional condition is imposed, which defines the observation gain $\phi_i(x)$ in terms of the transformation kernel $\Phi_i(x,y)$.

$$\phi_i(x) = -\varepsilon_i \Phi_i(x,0) \tag{131}$$

Lemma 7. *The Klein-Gordon PDEs defined by* (128)-(130) *admit unique $C^2(\mathcal{T})$ solutions. As a direct result, the gain kernels ϕ_i are bounded in the domain $\mathcal{T}$, that is,*

$$||\Phi_i||_{L^\infty} := \max_{(x,y)\in\mathcal{T}} |\Phi_i(x,y)| \leq \bar{\Phi}_i < \infty \tag{132}$$

The proof of Lemma (7) is given in [16].

Remark. *For the special case $\lambda_i(x) = \lambda_i$ is a constant, an explicit solution to* (128)-(130) *can be found:*

$$\Phi_i(x,y) = -\frac{\lambda_i + c_i}{\varepsilon_i}(1-x)\frac{I_1(z)}{z} \tag{133}$$

$$z = \sqrt{\frac{\lambda_i + c_i}{\varepsilon_i}(2-x-y)} \tag{134}$$

where $I_1(z)$ is the modified Bessel function of the first kind.

IV. Kernel PDE well-posedness for (K,p,q,r)

A necessary and sufficient condition for the invertibility of (25), (33) (and their respective inverse transforms) is the existence of bounded kernels K,p,q on their respective domains. It is not trivially obvious that the kernel PDEs (96)-(99), (110),(111) are well-posed. The goal of this section is to establish and characterize the existence and uniqueness (and regularity) properties of these kernel PDEs.

A. Well-posedness of K

For K, we note that the kernel PDE is very similar to that of [22], and thus apply an adjusted approach to (96)-(98), (104). We use the following definition:

$$\check{K}(x,y) = \sqrt{E}\partial_x K(x,y) + \partial_y K(x,y)\sqrt{E} \tag{135}$$

which allows us to transform the 2×2 system of 2nd-order hyperbolic PDE K into the following $2\times 2\times 2$ 1st-order hyperbolic PDE system $(K,\check{K})$. Due to G possessing triangular structure (31) (a result of Assumption 1), we can separate the kernel PDEs into cascading sets of PDE systems.

1) Well-posedness of first row $\mathsf{K},\check{\mathsf{K}}$*: (*$\mathsf{k}_{1\mathrm{i}},\check{\mathsf{k}}_{1\mathrm{i}}$*):* The first set of kernel PDEs we study is $(k_{11},k_{12},\check{k}_{11},\check{k}_{12})$. These kernels comprise an autonomous system of first-order hyperbolic PDEs on a bounded triangular domain, and are *linear and x-invariant* PDEs. Thus, our expectation is that the energy of a (potentially weak) solution can only grow (in x) at an exponential rate at best.

The component-wise kernels are

$$\sqrt{\varepsilon_1}\partial_x k_{11}(x,y) + \sqrt{\varepsilon_1}\partial_y k_{11}(x,y) = \check{k}_{11}(x,y) \tag{136}$$

$$\sqrt{\varepsilon_1}\partial_x k_{12}(x,y) + \sqrt{\varepsilon_2}\partial_y k_{12}(x,y) = \check{k}_{12}(x,y) \tag{137}$$

$$\sqrt{\varepsilon_1}\partial_x \check{k}_{11}(x,y) - \sqrt{\varepsilon_1}\partial_y \check{k}_{11}(x,y) = (\lambda_1(y)+c_1)k_{11}(x,y) \tag{138}$$

$$\sqrt{\varepsilon_1}\partial_x \check{k}_{12}(x,y) - \sqrt{\varepsilon_2}\partial_y \check{k}_{12}(x,y) = (\lambda_2(y)+c_1)k_{12}(x,y) \tag{139}$$

with boundary conditions

$$k_{11}(x,0) = \frac{1}{2\varepsilon_1}\int_0^x \sqrt{\varepsilon_1}\check{k}_{11}(y,0) + \sqrt{\varepsilon_2}\check{k}_{12}(y,0)dy \tag{140}$$

$$k_{12}(x,0) = \frac{1}{2\sqrt{\varepsilon_1\varepsilon_2}}\int_0^x \sqrt{\varepsilon_1}\check{k}_{11}(y,0) + \sqrt{\varepsilon_2}\check{k}_{12}(y,0)dy \tag{141}$$

$$k_{12}(x,x) = 0 \tag{142}$$

$$\check{k}_{11}(x,x) = -\frac{\lambda_1(x)+c_1}{2\sqrt{\varepsilon_1}} \tag{143}$$

$$\check{k}_{12}(x,x) = 0 \tag{144}$$

The system of kernel equations $(k_{1i},\check{k}_{1i})$ is self contained. Due to Assumption 1, the characteristics of the kernel equations $k_{12},\check{k}_{12}$ will have sub-unity slope, in turn neccessitating two boundary condtions on k_{12} at the $y=0$ and $y=x$ boundaries.

Lemma 8. *The system of first-order hyperbolic PDEs* (136)-(139) *and associated boundary conditions admit a unique set of $k_{11},k_{12}\in C^2(\mathcal{T})$, $\check{k}_{11},\check{k}_{12}\in C^1(\mathcal{T})$ solutions.*

Proof. With a direct application of the method of characteristics to (136)-(139), Volterra-type integral equations can be recovered:

$$k_{11}(x,y) = \frac{1}{2\varepsilon_1}\int_0^{x-y} \sqrt{\varepsilon_1}\check{k}_{11}(z,0) + \sqrt{\varepsilon_2}\check{k}_{12}(z,0)dz + \int_0^{\sqrt{\varepsilon_1^{-1}}y} \check{k}_{11}(\sqrt{\varepsilon_1}z + x - y, \sqrt{\varepsilon_1}z)dz \tag{145}$$

$$k_{12}(x,y) = \begin{cases} k_{12,l} & \sqrt{\varepsilon_1}y \leq \sqrt{\varepsilon_2}x \\ k_{12,u} & \sqrt{\varepsilon_1}y \geq \sqrt{\varepsilon_2}x \end{cases} \tag{146}$$

$$\check{k}_{11}(x,y) = -\frac{\lambda_1\left(\frac{x+y}{2}\right)+c_1}{2\sqrt{\varepsilon_1}} + \int_0^{\frac{x-y}{2\sqrt{\varepsilon_1}}} \left(\lambda_1\left(-\sqrt{\varepsilon_1}z + \frac{x+y}{2}\right)+c_1\right) \times k_{11}\left(\sqrt{\varepsilon_1}z + \frac{x+y}{2}, -\sqrt{\varepsilon_1}z + \frac{x+y}{2}\right)dz \tag{147}$$

$$\check{k}_{12}(x,y) = \int_0^{\frac{x-y}{\sqrt{\varepsilon_1}+\sqrt{\varepsilon_2}}} \lambda_2(-\sqrt{\varepsilon_2}z + \sigma_3(x,y) + c_1) \times k_{12}(\sqrt{\varepsilon_1}z + \sigma_3(x,y), -\sqrt{\varepsilon_2}z + \sigma_3(x,y))dz \tag{148}$$

where $k_{12,u},k_{12,l}$ is defined by

$$k_{12,l}(x,y) = \frac{1}{2\sqrt{\varepsilon_1\varepsilon_2}}\int_0^{\sigma_1(x,y)} \sqrt{\varepsilon_1}\check{k}_{11}(z,0) + \sqrt{\varepsilon_2}\check{k}_{12}(z,0)dz + \int_0^{\sqrt{\varepsilon_2^{-1}}y} \check{k}_{12}(\sqrt{\varepsilon_1}z + \sigma_1(x,y), \sqrt{\varepsilon_2}z)dz \tag{149}$$

$$k_{12,u}(x,y) = \int_0^{\frac{x-y}{\sqrt{\varepsilon_1}-\sqrt{\varepsilon_2}}} \check{k}_{12}(\sqrt{\varepsilon_1}z + \sigma_2(x,y),$$

$$\sqrt{\varepsilon_2}z + \sigma_2(x,y))dz \tag{150}$$

and the functions σ_i given by

$$\sigma_1(x,y) = \sqrt{\varepsilon_2^{-1}}(\sqrt{\varepsilon_2}x - \sqrt{\varepsilon_1}y) \tag{151}$$
$$\sigma_2(x,y) = (\sqrt{\varepsilon_1} - \sqrt{\varepsilon_2})^{-1}(\sqrt{\varepsilon_1}y - \sqrt{\varepsilon_2}x) \tag{152}$$
$$\sigma_3(x,y) = (\sqrt{\varepsilon_1} + \sqrt{\varepsilon_2})^{-1}(\sqrt{\varepsilon_2}x + \sqrt{\varepsilon_1}y) \tag{153}$$

From substituting (148) into (146) on the domain $\mathcal{T}' := \{(x,y) \in \mathbb{R}^2 | 0 \leq \sqrt{\varepsilon_2/\varepsilon_1}x \leq y \leq x \leq 1\}$, one can immediately notice $k_{12,u}(x,y) = \check{k}_{12}(x,y) \equiv 0, (x,y) \in \mathcal{T}'$.

Using (145)-(148), the following integral equation relations can be established:

$$\begin{pmatrix} k_{11} \\ k_{12} \end{pmatrix} = \Gamma_1 \left[\begin{pmatrix} \check{k}_{11} \\ \check{k}_{12} \end{pmatrix} \right] := I_1 \left[\begin{pmatrix} \check{k}_{11} \\ \check{k}_{12} \end{pmatrix} \right] (x,y) + \Psi_1(x,y) \tag{154}$$

$$\begin{pmatrix} \check{k}_{11} \\ \check{k}_{12} \end{pmatrix} = \Gamma_2 \left[\begin{pmatrix} k_{11} \\ k_{12} \end{pmatrix} \right] := I_2 \left[\begin{pmatrix} k_{11} \\ k_{12} \end{pmatrix} \right] (x,y) + \Psi_2(x,y) \tag{155}$$

where the operators Γ_1, Γ_2 over $(x,y) \in \mathcal{T})$ encapsulate the affine integral equations (145)-(148), and I_1, I_2 represent the linear part in $k, \check{k}$, while Ψ_1, Ψ_2 represent the constant part. We establish the following iteration via the method of successive approximations to recover a solution:

$$\begin{pmatrix} k_{11,n+1} \\ k_{12,n+1} \end{pmatrix} = (\Gamma_1 \circ \Gamma_2) \left[\begin{pmatrix} k_{11,n} \\ k_{12,n} \end{pmatrix} \right] \tag{156}$$

The existence of a solution (k_{11}, k_{12}) through the iteration (156) will imply the existence of a solution $(\check{k}_{11}, \check{k}_{12})$ via (155). To show that this iteration converges, we first define

$$\Delta k_{1,n} := \begin{pmatrix} \Delta k_{11,n} \\ \Delta k_{12,n} \end{pmatrix} := \begin{pmatrix} k_{11,n+1} - k_{11,n} \\ k_{12,n+1} - k_{12,n} \end{pmatrix} \tag{157}$$

Applying (157) to (156) and utilizing the properties of affine operators, one can recover the following iteration for $\Delta k_{1,n}$:

$$\Delta k_{1,n+1} = (I_1 \circ I_2)[\Delta k_{1,n}](x,y) \tag{158}$$

As $\Gamma_1 \circ \Gamma_2$ is a continuous mapping over the complete convex space of bounded continuous functions, then the following statement holds via the Schauder fixed point theorem.

$$\lim_{n\to\infty} \begin{pmatrix} k_{11,n} \\ k_{12,n} \end{pmatrix} = \begin{pmatrix} k_{11,0} \\ k_{12,0} \end{pmatrix} + \sum_{n=0}^{\infty} \Delta k_{1,n} = \begin{pmatrix} k_{11} \\ k_{12} \end{pmatrix} \tag{159}$$

Choosing $k_{11,0} = k_{12,0} = 0$, one can compute the following bound on $\Delta k_{1,0}$ directly:

$$||\Delta k_{1,0}||_1 \leq \left(\frac{\bar{\lambda} + c_1}{2\sqrt{\varepsilon_1\varepsilon_2}} \right) x \tag{160}$$

where we have taken the liberty of defining

$$\bar{\lambda} := \max\{||\lambda_1||_{L^\infty}, ||\lambda_2||_{L^\infty}\} = ||\lambda||_{L^\infty} \tag{161}$$

It is important to note that the norm $||\Delta k_{1,0}||_1$ is the *vector* 1-norm and not the L^1 function norm. That is,

$$||\Delta k_{1,n}||_1 := |\Delta k_{11,n}(x,y)| + |\Delta k_{12,n}(x,y)| \tag{162}$$

By using (160) in (158), one can find the following bound on $||\Delta k_{1,n}||_1$ indexed by iteration n:

$$||\Delta k_{1,n}||_1 \leq \frac{2^n}{(2n+1)!} \left(\frac{\bar{\lambda} + c_1}{2\sqrt{\varepsilon_1\varepsilon_2}} \right)^{n+1} x^{2n+1} \tag{163}$$

Due to the bounded domain $\mathcal{T}$, one can find *uniform* convergence properties (where the uniform bound is simply evaluated for $x^{2n+1} \leq 1, \forall x \in [0,1]$). From (159),

$$\left|\left| \begin{pmatrix} k_{11} \\ k_{12} \end{pmatrix} \right|\right|_1 \leq \sum_{n=0}^{\infty} \frac{2^n}{(2n+1)!} \left(\frac{\bar{\lambda} + c_1}{2\sqrt{\varepsilon_1\varepsilon_2}} \right)^{n+1} x^{2n+1} \tag{164}$$

To recover the $C^2(\mathcal{T})$ regularity, one can directly reference (159). Noting that the set $C^n(\mathcal{T})$ is closed under addition for $n \in \mathbb{N}$ along with the *integral* iteration (158), it is easy to see that $\lambda_1, \lambda_2 \in C^1([0,1])$ generates the regularity $k_{11}, k_{12} \in C^2(\mathcal{T})$. □

2) Well-posedness of second row $\mathsf{K}, \check{\mathsf{K}}$: ($\mathsf{k}_{2i}, \check{\mathsf{k}}_{2i}$): The second set of kernels is $(k_{21}, k_{22}, \check{k}_{21}, \check{k}_{22})$. These feature the kernels k_{11}, k_{12} acting as source terms, however, by employing estimates of k_{11}, k_{12} from Lemma 8, we can simplify the system significantly. However, the structure of the problem is different, most notably in how the characteristics evolve.

To account for the different nature of these characteristics, we perform one more transformation on the kernels for k_{2i}:

$$\hat{k}_{2i}(x,y) = \sqrt{\varepsilon_2}\partial_x k_{2i}(x,y) - \sqrt{\varepsilon_i}\partial_y k_{2i}(x,y) \tag{165}$$

where $i \in \{1,2\}$. We then turn our attention to the gain kernel system $(\hat{k}_{21}, \check{k}_{21}, \hat{k}_{22}, \check{k}_{22})$.

The component system of kernel PDEs for $(\hat{k}_{21}, \check{k}_{21}, \hat{k}_{22}, \check{k}_{22})$ is

$$\sqrt{\varepsilon_2}\partial_x \hat{k}_{21}(x,y) + \sqrt{\varepsilon_1}\partial_y \hat{k}_{21}(x,y) = (\lambda_1(y) + c_2)k_{21}(x,y) - g[k_{21}](x)k_{11}(x,y) \tag{166}$$

$$\sqrt{\varepsilon_2}\partial_x \hat{k}_{22}(x,y) + \sqrt{\varepsilon_2}\partial_y \hat{k}_{22}(x,y) = (\lambda_2(y) + c_2)k_{22}(x,y) - g[k_{21}](x)k_{12}(x,y) \tag{167}$$

$$\sqrt{\varepsilon_2}\partial_x \check{k}_{21}(x,y) - \sqrt{\varepsilon_1}\partial_y \check{k}_{21}(x,y) = (\lambda_1(y) + c_2)k_{21}(x,y) - g[k_{21}](x)k_{11}(x,y) \tag{168}$$

$$\sqrt{\varepsilon_2}\partial_x \check{k}_{22}(x,y) - \sqrt{\varepsilon_2}\partial_y \check{k}_{22}(x,y) = (\lambda_2(y) + c_2)k_{22}(x,y) - g[k_{21}](x)k_{12}(x,y) \tag{169}$$

subject to the following boundary conditions:

$$\hat{k}_{21}(x,0) = a\check{k}_{22}(x,0) \tag{170}$$
$$\hat{k}_{22}(x,0) = a^{-1}\check{k}_{21}(x,0) \tag{171}$$
$$\check{k}_{21}(x,x) = -\frac{\sqrt{\varepsilon_1} - \sqrt{\varepsilon_2}}{\sqrt{\varepsilon_1} + \sqrt{\varepsilon_2}}\hat{k}_{21}(x,x) \tag{172}$$
$$\check{k}_{22}(x,x) = -\frac{\lambda_2(x) + c_2}{2\sqrt{\varepsilon_2}} \tag{173}$$

where the inverse transformations are given to be

$$k_{21}(x,y) = \frac{1}{2\sqrt{\varepsilon_2}} \int_y^x \check{k}_{21}(z,y) + \hat{k}_{21}(z,y)dz \tag{174}$$

$$k_{22}(x,y) = -\int_0^y \frac{\lambda_2(z)+c_2}{2\sqrt{\varepsilon_2}}dz + \frac{1}{2\sqrt{\varepsilon_2}}\int_y^x \check{k}_{22}(z,y)+\hat{k}_{22}(z,y)dz \quad (175)$$

and the function $g[k_{21}](x)$ can be expressed in terms of $\hat{k}_{21}, \check{k}_{21}$:

$$g[k_{21}](x) = \frac{(\varepsilon_2-\varepsilon_1)}{2\sqrt{\varepsilon_1}}(\check{k}_{21}(x,x)-\hat{k}_{21}(x,x)) \quad (176)$$

Without the estimates given by Lemma 8, the system of gain kernels would in fact be *nonlinear*, a significantly harder problem.

Lemma 9. *The system of first-order hyperbolic PDEs* (166)-(169) *and associated boundary conditions admit a unique set of* $\hat{k}_{21}, \check{k}_{21}, \hat{k}_{22}, \check{k}_{22} \in C^1(\mathcal{T})$ *solutions.*

Proof. The primary technical difficulty of this proof is incorporating the trace term $g[k_{21}](x)$. While in standard integral equation solutions one can apply successive approximations to recover a convergent sum of monomial terms (in increasing powers), the trace term $g[k_{21}](x)$ presents additional complexity with this approach.

We apply the method of characteristics to (166)-(169) to recover the following system of coupled integro-algebraic equations:

$$\hat{k}_{21}(x,y) = \hat{k}_{21}(\sigma_4(x,y),0) + \hat{I}_{21}[\hat{k}_{21},\check{k}_{21}](x,y) \quad (177)$$

$$\hat{k}_{22}(x,y) = \hat{k}_{22}(x-y,0) + \hat{I}_{22}[\hat{k}_{22},\check{k}_{22},\hat{k}_{21}](x,y) - \int_0^{\frac{y}{\sqrt{\varepsilon_2}}}\left[\frac{\lambda_2(\sqrt{\varepsilon_2}z)+c_2}{2\sqrt{\varepsilon_2}} \times \int_0^{\sqrt{\varepsilon_2}z}(\lambda_2(\xi)+c_2)d\xi\right]dz \quad (178)$$

$$\check{k}_{21}(x,y) = \check{k}_{21}(\sigma_5(x,y),\sigma_5(x,y)) + \check{I}_{21}[\hat{k}_{21},\check{k}_{21}](x,y) \quad (179)$$

$$\check{k}_{22}(x,y) = \check{k}_{22}\left(\frac{x+y}{2},\frac{x+y}{2}\right) + \check{I}_{22}[\hat{k}_{22},\check{k}_{22},\hat{k}_{21}](x,y) - \int_0^{\frac{x-y}{2\sqrt{\varepsilon_2}}}\left[\frac{\lambda_2\left(-\sqrt{\varepsilon_2}z+\frac{x+y}{2}\right)+c_2}{2\sqrt{\varepsilon_2}} \times \int_0^{-\sqrt{\varepsilon_2}z+\frac{x+y}{2}}(\lambda_2(\xi)+c_2)d\xi\right]dz \quad (180)$$

where

$$\sigma_4(x,y) := x - \frac{\sqrt{\varepsilon_2}}{\sqrt{\varepsilon_1}}y \quad (181)$$

$$\sigma_5(x,y) := \frac{\sqrt{\varepsilon_1}x+\sqrt{\varepsilon_2}y}{\sqrt{\varepsilon_1}+\sqrt{\varepsilon_2}} \quad (182)$$

and the integral operators $\hat{I}_{21}, \hat{I}_{22}, \check{I}_{21}, \check{I}_{22}$ are defined

$$\hat{I}_{21}[\hat{k}_{21},\check{k}_{21}](x,y) := \int_0^{\frac{y}{\sqrt{\varepsilon_1}}}\Bigg[-\frac{\varepsilon_2-\varepsilon_1}{\sqrt{\varepsilon_1}+\sqrt{\varepsilon_2}}k_{11}(\sqrt{\varepsilon_2}z+\sigma_4(x,y),\sqrt{\varepsilon_1}z) \times \hat{k}_{21}(\sqrt{\varepsilon_2}z+\sigma_4(x,y),\sqrt{\varepsilon_2}+\sigma_4(x,y)) + \frac{\lambda_1(\sqrt{\varepsilon_1}z)+c_2}{2\sqrt{\varepsilon_2}}\int_{\sqrt{\varepsilon_1}z}^{\sqrt{\varepsilon_2}z+\sigma_4(x,y)}\Big(\check{k}_{21}(\xi,\sqrt{\varepsilon_1}z) + \hat{k}_{21}(\xi,\sqrt{\varepsilon_1}z)\Big)d\xi\Bigg]dz \quad (183)$$

$$\hat{I}_{22}[\hat{k}_{22},\check{k}_{22},\hat{k}_{21}](x,y) := \int_0^{\frac{y}{\sqrt{\varepsilon_2}}}\Bigg[-\frac{\varepsilon_2-\varepsilon_1}{\sqrt{\varepsilon_1}+\sqrt{\varepsilon_2}}k_{12}(\sqrt{\varepsilon_2}z+x-y,\sqrt{\varepsilon_2}z) \times \hat{k}_{21}(\sqrt{\varepsilon_2}z+x-y,\sqrt{\varepsilon_2}+x-y) + \frac{\lambda_2(\sqrt{\varepsilon_2}z)+c_2}{2\sqrt{\varepsilon_2}}\Bigg(\int_{\sqrt{\varepsilon_2}z}^{\sqrt{\varepsilon_2}z+x-y}\Big(\check{k}_{22}(\xi,\sqrt{\varepsilon_2}z) + \hat{k}_{22}(\xi,\sqrt{\varepsilon_2}z)\Big)d\xi\Bigg)\Bigg]dz \quad (184)$$

$$\check{I}_{21}[\hat{k}_{21},\check{k}_{21}](x,y) := \int_0^{\frac{x-y}{\sqrt{\varepsilon_1}+\sqrt{\varepsilon_2}}}\Bigg[-\frac{\varepsilon_2-\varepsilon_1}{\sqrt{\varepsilon_1}+\sqrt{\varepsilon_2}}k_{11}(\sqrt{\varepsilon_2}z+\sigma_5(x,y), -\sqrt{\varepsilon_1}z+\sigma_5(x,y)) \times \hat{k}_{21}(\sqrt{\varepsilon_2}z+\sigma_5(x,y),\sqrt{\varepsilon_2}+\sigma_5(x,y)) + \frac{\lambda_1(-\sqrt{\varepsilon_1}z+\sigma_5(x,y))+c_2}{2\sqrt{\varepsilon_2}} \times \int_{-\sqrt{\varepsilon_1}z+\sigma_5(x,y)}^{\sqrt{\varepsilon_2}z+\sigma_5(x,y)}\Big(\check{k}_{21}(\xi,-\sqrt{\varepsilon_1}z+\sigma_5(x,y)) + \hat{k}_{21}(\xi,-\sqrt{\varepsilon_1}z+\sigma_5(x,y))\Big)d\xi\Bigg]dz \quad (185)$$

$$\check{I}_{22}[\hat{k}_{22},\check{k}_{22},\hat{k}_{21}](x,y) := \int_0^{\frac{x-y}{2\sqrt{\varepsilon_2}}}\Bigg[-\frac{\varepsilon_2-\varepsilon_1}{\sqrt{\varepsilon_1}+\sqrt{\varepsilon_2}} \times k_{12}\left(\sqrt{\varepsilon_2}z+\frac{x+y}{2},-\sqrt{\varepsilon_2}z+\frac{x+y}{2}\right) \times \hat{k}_{21}\left(\sqrt{\varepsilon_2}z+\frac{x+y}{2},\sqrt{\varepsilon_2}+\frac{x+y}{2}\right) + \frac{\lambda_2\left(-\sqrt{\varepsilon_2}z+\frac{x+y}{2}\right)+c_2}{2\sqrt{\varepsilon_2}} \times \Bigg(\int_{-\sqrt{\varepsilon_2}z+\frac{x+y}{2}}^{\sqrt{\varepsilon_2}z+\frac{x+y}{2}}\left(\check{k}_{22}\left(\xi,-\sqrt{\varepsilon_2}z+\frac{x+y}{2}\right) + \hat{k}_{21}\left(\xi,-\sqrt{\varepsilon_2}z+\frac{x+y}{2}\right)\right)d\xi\Bigg)\Bigg]dz \quad (186)$$

From enforcing (170)-(173) on (177)-(180), one can eventually arrive at an integral equation system representation for $(\hat{k}_{21},\hat{k}_{22},\check{k}_{21},\check{k}_{22})$. The integral equations can be separated into two groups of terms – an affine term and a linear integral operator term.

$$\hat{k}_{21}(x,y) = a\Bigg[-\frac{1}{2\sqrt{\varepsilon_2}}\left(\lambda_2\left(\frac{1}{2}\sigma_4(x,y)\right)+c_2\right)$$

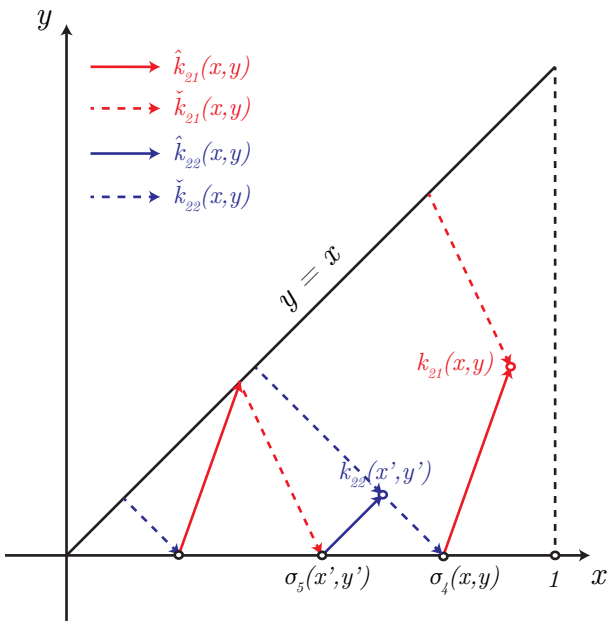

Fig. 2. Characteristics of $\hat{k}_{21}, \hat{k}_{22}, \check{k}_{21}, \check{k}_{22}$. Due to the unit slope of the $\hat{k}_{22}, \check{k}_{22}$ characteristics and reflection boundaries at $y = 0, y = x$, a maximum of 3 reflections (encompassing 4 characteristics) will occur.

$$
\begin{aligned}
&- \int_0^{\frac{\sigma_4(x,y)}{2\sqrt{\varepsilon_2}}} \left(\frac{1}{2\sqrt{\varepsilon_2}} \left(\lambda_2 \left(-\sqrt{\varepsilon_2} z + \frac{1}{2}\sigma_4(x,y) \right) + c_2 \right) \right. \\
&\qquad \left. \times \int_0^{-\sqrt{\varepsilon_2} z + \frac{1}{2}\sigma_4(x,y)} (\lambda_2(\xi) + c_2) d\xi \right) dz \\
&\quad + \check{I}_{22}[\hat{k}_{22}, \check{k}_{22}, \hat{k}_{21}] \Big] \\
&\quad + \hat{I}_{21}[\hat{k}_{21}, \check{k}_{21}](x,y) \qquad (187)
\end{aligned}
$$

$$
\begin{aligned}
&\hat{k}_{22}(x,y) = \\
&\delta_1 \left(\frac{1}{2\sqrt{\varepsilon_2}} (\lambda_2(\delta_1(x-y)) + c_2) \right. \\
&\quad - \int_0^{\frac{1}{2\sqrt{\varepsilon_2}}(x-y)} \frac{1}{2\sqrt{\varepsilon_2}} (\lambda_2(-\sqrt{\varepsilon_2} z + \frac{1}{2}\delta_1(x-y)) + c_2) \\
&\qquad \left. \times \int_0^{-\sqrt{\varepsilon_2} z + \frac{1}{2}\delta_1(x-y)} (\lambda_2(\xi) + c_2) d\xi dz \right) \\
&\quad + a^{-1} \hat{I}_{21}[\hat{k}_{21}, \check{k}_{21}](\delta_2(x-y)) \\
&\quad + \check{I}_{22}[\hat{k}_{22}, \check{k}_{22}, \hat{k}_{21}](\delta_1(x-y), 0) \\
&\quad + a^{-1} \check{I}_{21}[\hat{k}_{21}, \check{k}_{21}](x-y, 0) + \hat{I}_{22}[\hat{k}_{22}, \check{k}_{22}, \hat{k}_{21}](x,y) \\
&\quad - \int_0^{\frac{y}{\sqrt{\varepsilon_2}}} \frac{1}{2\sqrt{\varepsilon_2}} (\lambda_2(\sqrt{\varepsilon_2} z) + c_2) \\
&\qquad \times \int_0^{\sqrt{\varepsilon_2} z} (\lambda_2(\xi) + c_2) d\xi dz \qquad (188)
\end{aligned}
$$

$$
\begin{aligned}
&\check{k}_{21}(x,y) = \\
&- \delta_1 \left(a \left(- \frac{1}{2\sqrt{\varepsilon_2}} (\lambda_2(\delta_1(x + \frac{\sqrt{\varepsilon_2}}{\sqrt{\varepsilon_1}} y)) + c_2) \right. \right. \\
&\quad - \int_0^{\frac{\delta_1}{2\sqrt{\varepsilon_2}}(x + \frac{\sqrt{\varepsilon_2}}{\sqrt{\varepsilon_1}} y)} \frac{1}{2\sqrt{\varepsilon_2}} \left(\lambda_2(-\sqrt{\varepsilon_2} z + \frac{1}{2}\delta_1(x + \frac{\sqrt{\varepsilon_2}}{\sqrt{\varepsilon_1}} y)) \right. \\
&\qquad \left. + c_2 \right) \\
&\qquad \left. \times \int_0^{-\sqrt{\varepsilon_2} z + \frac{1}{2}\delta_1(x + \frac{\sqrt{\varepsilon_2}}{\sqrt{\varepsilon_1}} y)} (\lambda_2(\xi) + c_2) d\xi dz \right) \\
&\quad + \hat{I}_{21}[\hat{k}_{21}, \check{k}_{21}](\sigma_5(x,y), \sigma_5(x,y)) \\
&\quad + a \hat{I}_{22}[\hat{k}_{22}, \check{k}_{22}, \hat{k}_{21}](\delta_1(x + \frac{\sqrt{\varepsilon_2}}{\sqrt{\varepsilon_1}} y), \delta_1(x + \frac{\sqrt{\varepsilon_2}}{\sqrt{\varepsilon_1}} y)) \Big) \\
&\quad + \check{I}_{21}[\hat{k}_{21}, \check{k}_{21}](x,y) \qquad (189)
\end{aligned}
$$

$$
\begin{aligned}
&\check{k}_{22}(x,y) = \\
&- \frac{\lambda_2(\frac{x+y}{2}) + c_2}{2\sqrt{\varepsilon_2}} + \check{I}_{22}[\hat{k}_{22}, \check{k}_{22}, \hat{k}_{21}](x,y) \\
&- \int_0^{\frac{x-y}{2\sqrt{\varepsilon_2}}} \left[\frac{\lambda_2 \left(-\sqrt{\varepsilon_2} z + \frac{x+y}{2} \right) + c_2}{2\sqrt{\varepsilon_2}} \right. \\
&\qquad \left. \times \int_0^{-\sqrt{\varepsilon_2} z + \frac{x+y}{2}} (\lambda_2(\xi) + c_2) d\xi \right] dz \qquad (190)
\end{aligned}
$$

where δ_1, δ_2 are defined

$$\delta_1 = \frac{\sqrt{\varepsilon_1} - \sqrt{\varepsilon_2}}{\sqrt{\varepsilon_1} + \sqrt{\varepsilon_2}} \qquad (191)$$

$$\delta_2 = \frac{\sqrt{\varepsilon_1}}{\sqrt{\varepsilon_1} + \sqrt{\varepsilon_2}} \qquad (192)$$

Since $a < 1, \varepsilon_1 > \varepsilon_2$ as per Assumption 1, the coefficients $\delta_{1,2} \in (0,1)$. Due to the geometry of the characteristics, the kernels $\hat{k}_{21}, \hat{k}_{22}, \check{k}_{21}, \check{k}_{22}$ are coupled at the boundaries with at most 4 reflections. They are also coupled in domain through the trace term $g[k_{21}](x)$, and thus must be solved simultaneously.

Like in the proof of Lemma 8, we will define the integral equations (187)-(190) in terms of operators for notational compactness. Let $k_2 := (\hat{k}_{21}, \hat{k}_{22}, \check{k}_{21}, \check{k}_{22})$, and

$$k_2 = I_3[k_2](x,y) + \Psi_3(x,y) \qquad (193)$$

where I_3 is the operator involving the integral operators $\hat{I}_{2i}, \check{I}_{2i}$ while Ψ_3 collects the affine terms independent of $\hat{k}_{2i}, \check{k}_{2i}$. We establish an iteration $k_{2,n}$ as

$$k_{2,n+1} = I_3[k_{2,n}](x,y) + \Psi_3(x,y) \qquad (194)$$

with the iteration residual $\Delta k_{2,n} := k_{2,n+1} - k_{2,n}$ defining the iteration

$$\Delta k_{2,n+1} = I_3[\Delta k_{2,n}](x,y) \qquad (195)$$

We note that (193) is a continuous mapping over the complete (convex) metric space of bounded continuous functions (via the Schauder fixed point theorem), and make the following statement:

$$\lim_{n\to\infty} k_{2,n} = k_{2,0} + \sum_{n=0}^{\infty} \Delta k_{2,n} = k_2 \qquad (196)$$

Supposing that $k_{2,0} = 0$,

$$
\begin{aligned}
||\Delta k_{2,0}||_1 = ||\Psi_3||_1 \leq &\left(\frac{\bar{\lambda} + c_2}{2\sqrt{\varepsilon_2}} \right) (1 + a + \delta_1 + \delta_1 a) \\
&+ \frac{1}{2} \left(\frac{\bar{\lambda} + c_2}{2\sqrt{\varepsilon_2}} \right)^2 (6 + a + \delta_1 + 4a\delta_1^3)
\end{aligned}
$$

$$\leq \bar{\Psi}_{3,0} \tag{197}$$

From iterating $||\Delta k_{2,0}||_1$ through (195), one can achieve successive bounds on $\Delta k_{2,n}$:

$$||\Delta k_{2,n}||_1 \leq \frac{1}{n!}\left[\left((a^{-1}-1)\left|\left|\begin{pmatrix}k_{11}\\k_{12}\end{pmatrix}\right|\right|_{1,L^\infty}+\frac{\bar{\lambda}+c_2}{\varepsilon_2}\right)\times(8+2a+2a^{-1})\right]^n\bar{\Psi}_{3,0}x^n \tag{198}$$

Then, via (196) and noting $x \in [0,1]$, we can arrive at the following bound on k_2:

$$||k_2||_1 \leq \sum_{n=0}^{\infty}||\Delta k_{2,n}||_1 \tag{199}$$

which is the power series representation of an exponential bound. The regularity of the solution k_2 is also derived from (196), where noting that the initial choice of $k_{2,0}=0$ admits $\Delta k_{2,0}=\Psi_3$, which is $C^1(\mathcal{T})$ as it involves sums of $\lambda_2 \in C^1([0,1])$. Then from (174),(175), a single integration yields $k_{21}, k_{22} \in C^2(\mathcal{T})$. □

B. Well-posedness of p, q, r

As aformentioned, the (p,q,r)-system of kernel PDEs comprise a fairly interesting structure, the heart of which is a wave equation with an interface, whereby forcing is introduced via the differential transmission condition (113) at the interface. It is quite trivial to see that if one can show a solution exists for q, then necessarily, a solution p must exist as well.

To faciliate the study of the kernels, we will apply the Riemann invariant transformation as before found in the K kernel. As q,r share congruent characteristics, the solution method is much more straightforward and involves tracing characteristics through the square $\mathcal{T}\cup\mathcal{T}_{\mathrm{u}}$.

In this section, we have used the relation (110) to reduce the (p,q,r) system to (q,r), albeit at the cost of introducing trace terms into the q-PDE.

We begin by apply the following definition to derive the Rienmann invariants:

$$\hat{q}(x,y)=\sqrt{\varepsilon_2}\partial_x q(x,y)-\sqrt{\varepsilon_1}\partial_y q(x,y) \tag{200}$$
$$\check{q}(x,y)=\sqrt{\varepsilon_2}\partial_x q(x,y)+\sqrt{\varepsilon_1}\partial_y q(x,y) \tag{201}$$

which admit the following coupled PDEs for $(\hat{q},\check{q})$ defined on $\mathcal{T}$:

$$\sqrt{\varepsilon_2}\partial_x\hat{q}(x,y)+\sqrt{\varepsilon_1}\partial_y\hat{q}(x,y)=I_q[\hat{q},\check{q}](x,y) \tag{202}$$
$$\sqrt{\varepsilon_2}\partial_x\check{q}(x,y)-\sqrt{\varepsilon_1}\partial_y\check{q}(x,y)=I_q[\hat{q},\check{q}](x,y) \tag{203}$$

where the operator $I_q[\hat{q},\check{q}]$ is a linear integral operator defined as

$$I_q[\hat{q},\check{q}](x,y)=\frac{c_2-c_1}{2\sqrt{\varepsilon_2}}\int_0^x\check{q}(z,0)dz+\frac{c_2-c_1}{2\sqrt{\varepsilon_1}}\int_0^y(\check{q}(x,z)-\hat{q}(x,z))dz+\frac{a^{-1}g[k_{21}](y)}{2\sqrt{\varepsilon_2}}\int_0^{x-y}\check{q}(z,0)dz \tag{204}$$

In a similar manner, we define the Riemann invariants for r on $\mathcal{T}_{\mathrm{u}}$:

$$\hat{r}(x,y)=\sqrt{\varepsilon_2}\partial_x r(x,y)-\sqrt{\varepsilon_1}\partial_y r(x,y) \tag{205}$$
$$\check{r}(x,y)=\sqrt{\varepsilon_2}\partial_x r(x,y)+\sqrt{\varepsilon_1}\partial_y r(x,y) \tag{206}$$

which admits the coupled PDE:

$$\sqrt{\varepsilon_2}\partial_x\hat{r}(x,y)+\sqrt{\varepsilon_1}\partial_y\hat{r}(x,y)=I_r[\hat{r},\check{r}](x,y) \tag{207}$$
$$\sqrt{\varepsilon_2}\partial_x\check{r}(x,y)-\sqrt{\varepsilon_1}\partial_y\check{r}(x,y)=I_r[\hat{r},\check{r}](x,y) \tag{208}$$

where $I_r[\hat{r},\check{r}]$ is a linear integral operator defined as

$$I_r[\hat{r},\check{r}](x,y)=\frac{c_2-c_1}{2\sqrt{\varepsilon_2}}\int_0^x(\hat{r}(z,y)+\check{r}(z,y))dz \tag{209}$$

The PDEs given by (202),(203),(207),(208) are subject to the following boundary conditions, which consist of transmission and reflection boundary conditions:

$$\hat{q}(x,0)=0 \tag{210}$$
$$\check{q}(x,x)=\check{r}(x,x)-(\sqrt{\varepsilon_1}+\sqrt{\varepsilon_2})^{-1}g[k_{21}](x) \tag{211}$$
$$\hat{r}(0,y)=\check{r}(0,y)=\sqrt{\varepsilon_2}\left(\mathbf{1}_{\{y=0\}}(y)\frac{g[k_{21}](0)}{\varepsilon_2-\varepsilon_1}\right) \tag{212}$$
$$\hat{r}(x,x)=\hat{q}(x,x)-(\sqrt{\varepsilon_1}-\sqrt{\varepsilon_2})^{-1}g[k_{21}](x) \tag{213}$$
$$\check{r}(x,1)=-\hat{r}(x,1) \tag{214}$$

An additional condition employed implicity in the derivation of $(\hat{q},\check{q},\hat{r},\check{r})$ is the following point condition:

$$q(0,0)=r(0,0)=0 \tag{215}$$

Lemma 10. *The system of first-order hyperbolic PDE* (202),(203),(207),(208) *with associated boundary conditions colorblue admit a unique set of piecewise $C^1(\mathcal{T})$ solutions $(\hat{q},\check{q})$ and piecewise $C^1(\mathcal{T}_u)$ solutions $(\hat{r},\check{r})$.*

Proof. We can directly apply the method of characteristics to (202),(203),(207),(208) to recover the following linear integral equations:

$$\hat{q}(x,y)=\int_0^{\frac{y}{\sqrt{\varepsilon_1}}}I_q[\hat{q},\check{q}](\sigma_6(x,y)+\sqrt{\varepsilon_2}z,\sqrt{\varepsilon_1}z)dz \tag{216}$$

$$\check{q}(x,y)=\check{r}(\sigma_7(x,y),\sigma_7(x,y))-(\sqrt{\varepsilon_1}+\sqrt{\varepsilon_2})^{-1}g[k_{21}](\sigma_7(x,y))+\int_0^{\frac{x-y}{\sqrt{\varepsilon_1}+\sqrt{\varepsilon_2}}}I_q[\hat{q},\check{q}](\sqrt{\varepsilon_2}z+\sigma_7(x,y),-\sqrt{\varepsilon_1}z+\sigma_7(x,y))dz \tag{217}$$

where $\sigma_6,\sigma_7,\sigma_8$ are defined as

$$\sigma_6(x,y)=x-\sqrt{\frac{\varepsilon_2}{\varepsilon_1}}y \tag{218}$$
$$\sigma_7(x,y)=\frac{\sqrt{\varepsilon_1}x+\sqrt{\varepsilon_2}y}{\sqrt{\varepsilon_1}+\sqrt{\varepsilon_2}} \tag{219}$$

while for $\hat{r},\check{r}$, we recover piecewise defined linear integral equations which arises due to the mixing of initial and boundary conditions.

$$\hat{r}(x,y)=\begin{cases}\hat{r}_l(x,y) & x>\sqrt{\varepsilon_2/\varepsilon_1}y\\ \hat{r}_e(x,y) & x=\sqrt{\varepsilon_2/\varepsilon_1}y\\ 0 & x<\sqrt{\varepsilon_2/\varepsilon_1}y\end{cases} \tag{220}$$

$$\check{r}(x,y)=\begin{cases}\check{r}_u(x,y) & x\geq\sqrt{\varepsilon_2/\varepsilon_1}(2-y)\\ \check{r}_l(x,y) & \sqrt{\varepsilon_2/\varepsilon_1}y\leq x<\sqrt{\varepsilon_2/\varepsilon_1}(2-y)\\ 0 & x<\sqrt{\varepsilon_2/\varepsilon_1}y\end{cases} \tag{221}$$

where

$$\begin{aligned}\hat{r}_l(x,y)&=\hat{q}(\sigma_8(x,y),\sigma_8(x,y))\\&\quad-(\sqrt{\varepsilon_1}-\sqrt{\varepsilon_2})^{-1}g[k_{21}](\sigma_8(x,y))\\&\quad+\int_0^{\frac{y-x}{\sqrt{\varepsilon_1}-\sqrt{\varepsilon_2}}}I_r[\hat{r},\check{r}](\sqrt{\varepsilon_2}z+\sigma_8(x,y),\\&\qquad\sqrt{\varepsilon_1}z+\sigma_8(x,y))dz\end{aligned} \tag{222}$$

$$\begin{aligned}\hat{r}_e(x,y)&=\frac{g[k_{21}](0)}{\varepsilon_2-\varepsilon_1}\\&\quad-(\sqrt{\varepsilon_1}-\sqrt{\varepsilon_2})^{-1}g[k_{21}](\sigma_8(x,y))\\&\quad+\int_0^{\frac{y-x}{\sqrt{\varepsilon_1}-\sqrt{\varepsilon_2}}}I_r[\hat{r},\check{r}](\sqrt{\varepsilon_2}z+\sigma_8(x,y),\\&\qquad\sqrt{\varepsilon_1}z+\sigma_8(x,y))dz\end{aligned} \tag{223}$$

$$\begin{aligned}\check{r}_u(x,y)&=-\hat{r}(\sigma_9(x,y),1)\\&\quad+\int_0^{\frac{1-y}{\sqrt{\varepsilon_1}}}I_r[\hat{r},\check{r}](\sqrt{\varepsilon_2}z+\sigma_9(x,y),\\&\qquad-\sqrt{\varepsilon_1}z+1)dz\end{aligned} \tag{224}$$

$$\begin{aligned}\check{r}_l(x,y)&=\int_0^{\frac{\sqrt{\varepsilon_1}-\sqrt{\varepsilon_2}}{2\sqrt{\varepsilon_1}}}I_r[\hat{r},\check{r}](\sqrt{\varepsilon_2}z+\sigma_{10}(x,y),\\&\qquad-\sqrt{\varepsilon_1}z+\sigma_{10}(x,y))dz\end{aligned} \tag{225}$$

with $\sigma_8,\sigma_9,\sigma_{10}$ defned as

$$\sigma_8(x,y)=\frac{\sqrt{\varepsilon_1}x-\sqrt{\varepsilon_2}y}{\sqrt{\varepsilon_1}-\sqrt{\varepsilon_2}} \tag{226}$$

$$\sigma_9(x,y)=x+\sqrt{\frac{\varepsilon_2}{\varepsilon_1}}(y-1) \tag{227}$$

$$\sigma_{10}(x,y)=x+\sqrt{\frac{\varepsilon_2}{\varepsilon_1}}y \tag{228}$$

To study the well-posedness $\hat{q},\check{q},\hat{r},\check{r}$ system, it is helpful to study the characteristics geometrically, which are depicted in Figure 3.

Much like the analysis of the K kernel, we establish the following operator representation for the affine integral equations that govern $\rho:=(\hat{q},\check{q},\hat{r},\check{r})$:

$$\rho=\Gamma_3[\rho](x,y):=I_4[\rho](x,y)+\Psi_4(x,y) \tag{229}$$

where analogous to before, Γ_3 encapsulates the affine integral equations given by (216),(217),(220),(221). We separate the operator into the linear operator I_4 and the constant Ψ_4. Ψ_4 is evaluated to be

$$\Psi_4(x,y):=\begin{pmatrix}0 & \Psi_{4,1}(x,y) & \Psi_{4,2}(x,y) & \Psi_{4,3}(x,y)\end{pmatrix}^T \tag{230}$$

$$\begin{aligned}\Psi_{4,1}(x,y)&=(\sqrt{\varepsilon_1}-\sqrt{\varepsilon_2})^{-1}\\&\quad\times g[k_{21}](\sigma_8(\sigma_9(\sigma_7(x,y),\sigma_7(x,y)),1))\\&\quad-(\sqrt{\varepsilon_1}+\sqrt{\varepsilon_2})^{-1}g[k_{21}](\sigma_7(x,y))\\\Psi_{4,2}(x,y)&=-(\sqrt{\varepsilon_1}-\sqrt{\varepsilon_2})^{-1}g[k_{21}](\sigma_8(x,y))\\\Psi_{4,3}(x,y)&=(\sqrt{\varepsilon_1}-\sqrt{\varepsilon_2})^{-1}g[k_{21}](\sigma_8(\sigma_9(x,y),1))\end{aligned}$$

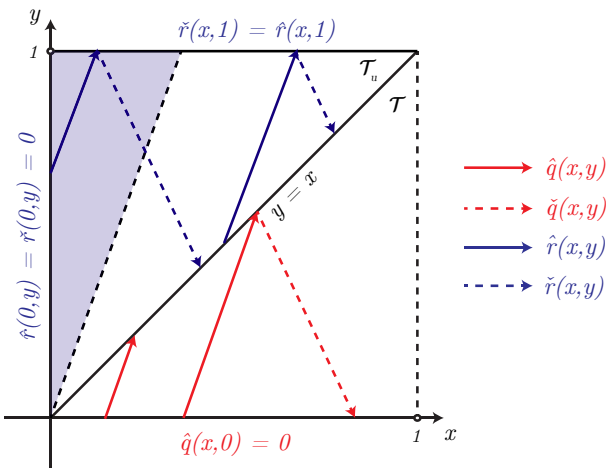

Fig. 3. Solution characteristics of $\hat{q},\check{q},\hat{r},\check{r}$. An interface between the solutions exists at $y=x$ defining a jump discontinuity. Because of the initial conditons imposed, $\hat{r}=\check{r}=0$ in the shaded triangle.

Intuitively, one can understand Ψ_4 to represent the nonzero data of the problem. If, perchance the folding point is chosen $y_0=0$, then $g[k_{21}]\equiv 0\Leftrightarrow\Psi_4\equiv 0$. It is precisely the unmatched artifact from the first transformation, $g[k_{21}]$, that acts as the sole forcing to the (q,r) PDE, as expected.

We carry out the same methodology as for K, and establish an iteration ρ_k for $n\in\mathbb{N}$:

$$\rho_{n+1}=I_4[\rho_n](x,y)+\Psi_4(x,y) \tag{231}$$

The residual $\Delta\rho_n:=\rho_{n+1}-\rho_n$ will obey the following linear integral equation,

$$\Delta\rho_n=I_4[\Delta\rho_n](x,y) \tag{232}$$

which arises from abusing the linear property of I_4. We note that in the complete space of bounded continuous functions, the iteration (231) will converge (via the Schauder fixed point theorem) if we can show uniform Cauchy convergence. The iteration limit thus can be rewritten as an infinite summation:

$$\lim_{n\to\infty}\rho_n=\rho_0+\sum_{n=0}^{\infty}\Delta\rho_n=\rho \tag{233}$$

It is quite clear from imposing (231),(232) that by choosing $\rho_0=0$, $\Delta\rho_0$ can be computed to be

$$\begin{aligned}&\Delta\rho_0=\Psi_4\\&\Rightarrow||\Delta\rho_0||_1=||\Psi_4||_1\leq\frac{4\sqrt{\varepsilon_1}+2\sqrt{\varepsilon_2}}{\varepsilon_1-\varepsilon_2}||g[k_{21}]||_{L^\infty}\end{aligned} \tag{234}$$

From using (234) in the iteration (232), one can find the successive bounds on the residuals:

$$||\Delta\rho_n||_1\leq\frac{1}{n!}\left(\frac{2\varepsilon_2^{-1}(2|c_1-c_2|+||g[k_{21}]||_{L^\infty}}{2}x\right)^n||\Psi_4||_1 \tag{235}$$

Noting (233), it is quite trivial to see that ρ is bounded (in vector 1-norm) by an exponential. This guarantees the existence of a solution ρ, and thus $(\hat{q},\check{q},\hat{r},\check{r})$ admit a solution. In fact, due to the linearity of the PDEs (202),(203),(207),(208), it is not difficult to show that this solution is also unique. □

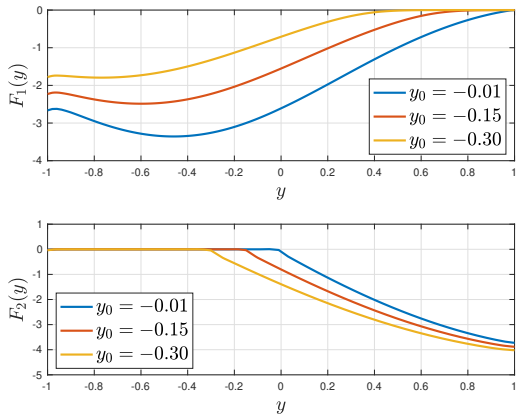

Fig. 4. Numerically computed gains for given reaction coefficient $\boldsymbol{\lambda(y)}$ for three separate folding cases. The folding cases encompasses different choices of control folding point $\boldsymbol{y_0}$.

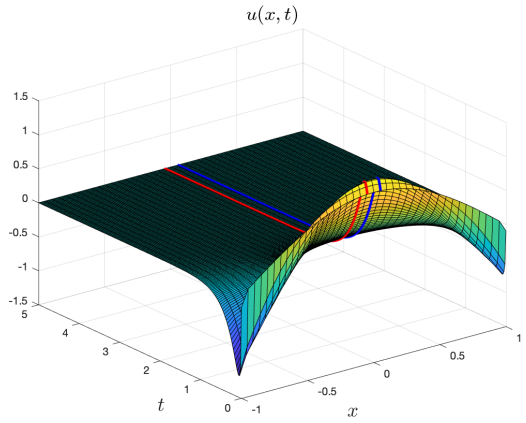

Fig. 5. Closed-loop response $\boldsymbol{u(x,t)}$ with folding points chosen to be $\boldsymbol{y_0 = -0.05, \hat{y}_0 = 0.05}$.

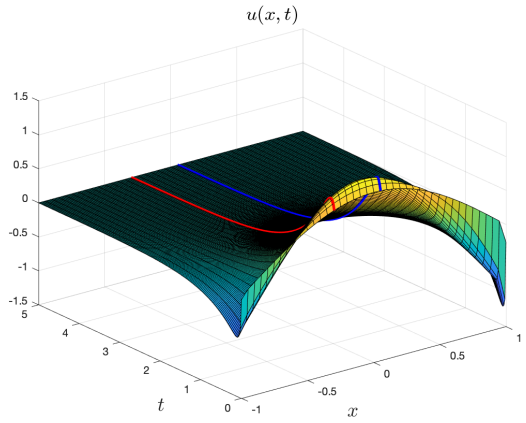

Fig. 6. Closed-loop response $\boldsymbol{u(x,t)}$ with folding points chosen to be $\boldsymbol{y_0 = -0.30, \hat{y}_0 = 0.05}$.

V. Folding point analysis and numerical study

The parameters chosen for simulation are given in Table I. λ is specifically chosen to not be symmetric about $x = 0$, and actually attains a maximum at $x = -0.25$. This is motivated by the intuition that choosing a folding point not at the point of symmetry $x = 0$ may afford better performance according a preferred index. It is also important to note that $c_1, c_2, \check{c}_1, \check{c}_2$ all influence the system response in some manner that is not wholly independent from the choices $y_0, \hat{y}_0$.

A. Folding point selection

It is difficult to directly characterize the size of the controller gains f_1, f_2 (defined in (45),(46)), but one may glean intuition for how the controllers grow based upon what the bounds on the gain kernels suggest.

As one may note from Figure 4, the control gains are not necessarily differentiable at the selected folding point. Surely, as $y_0 \to 0$ (the point of symmetry), one recovers the continuous, symmetric case. However, as the folding point is chosen to be more and more biased (for the same set of target system reaction coefficients c_i), it is clear to notice that one control gain grows smaller (implying less effort) while the other is magnified (implying more effort) – moreover, the domain of the state needed to be fed back varies as well.

Although not provable, the bounds (164),(199),(235) suggest this behavior as well. In (164), the bound on the controller gains k_{1i} arise as an exponential in $(a\varepsilon_1)^{-1}$. In (199),(235), the control gains k_{2i}, p, q are parametrized exponentially in $(a\varepsilon_2)^{-1}$. These bounds suggests that as one considers more biased folding points $y_0 \in (-1, 0)$, k_{1i} will decrease (i.e. less effort) while k_{2i} will increase (i.e. more effort).

Parameter	Value
ε	1
$\lambda(x)$	$-4x^2 - 2x + 6$
y_0	$-0.05, -0.30$
$\hat{y}_0$	$0.05, -0.45$
c_1, c_2	5
$\check{c}_1, \check{c}_2$	1

TABLE I
Simulation parameters

B. Numerical results for output-feedback

Due to the choice of a sufficiently large positive λ, the open-loop system is unstable and therefore necessitates feedback control. Two choices of control folding points y_0 and two choices of measurement points $\hat{y}_0$ are simulated, with the control folding point y_0 marked in red and the measurement point $\hat{y}_0$ marked in blue.

Comparing Figures 5, 7 with Figures 6,8 gives insight to how changing the control folding point affects the response – the controller $\mathcal{U}_1$ has a lower peak value in the biased case (Figure 6,8) than that of the close-to-symmetric case (Figure 5,7). However, it is quite clear to note that the controller $\mathcal{U}_2$ pays the cost in having a much higher peak value.

Comparing Figures 5,6 with Figures 7,8 gives insight to how changing the measurement point $\hat{y}_0$ affects the system response. Moving the folding point further away from the control folding may exhibit detrimental performance.

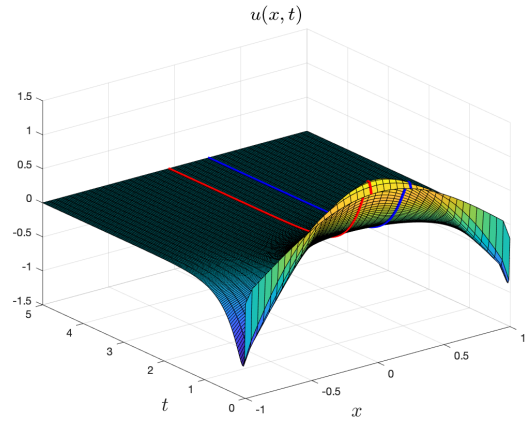

Fig. 7. Closed-loop response $\boldsymbol{u(x,t)}$ with folding points chosen to be $\boldsymbol{y_0 = -0.05, \hat{y}_0 = -0.45}$.

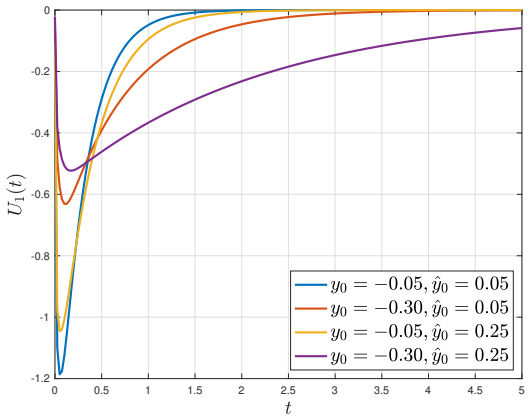

Fig. 9. Comparison of control effort by left controller ($\boldsymbol{\mathcal{U}_1(t)}$) over different folding choices

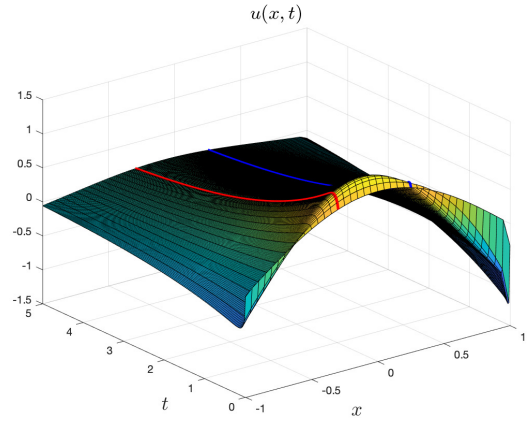

Fig. 8. Closed-loop response $\boldsymbol{u(x,t)}$ with folding points chosen to be $\boldsymbol{y_0 = -0.30, \hat{y}_0 = -0.45}$.

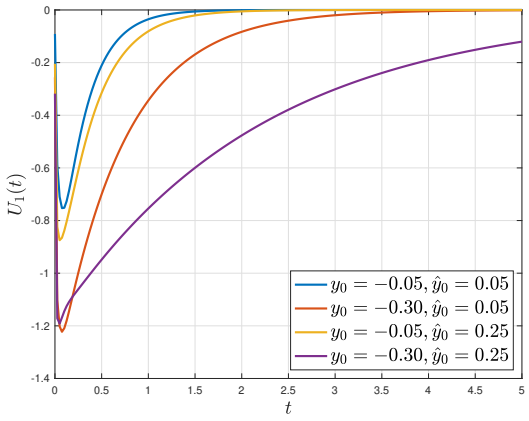

Fig. 10. Comparison of control effort by right controller ($\boldsymbol{\mathcal{U}_2(t)}$) over different folding choices

The controller responses are given in Figures 9,10. It can be noted that the selection of the control folding point appears to suggest an inherent waterbed effect in L^2 versus L^∞ (in time). The numerical simulations suggest that as $y_0 \to -1$ (the biased case), the controller improves in the L^2 sense at the cost of the peak value. Conversely, as $y_0 \to 0$ (the symmetric case), the controller improves in the L^∞ sense at the cost of the convergence speed (related to L^2).

VI. Conclusion

A methodology for designing output feedback bilateral boundary controllers for linear parabolic class PDEs is generated as the main result of the paper. Compared with existing bilateral control designs for parabolic PDEs, the folding appraoch affords additional design degrees of freedom in not only control but also observer design.

The primary advantage that the folding approach admits is a generalization of bilateral control design. A design for a given performance index e.g. energy (L^2) or boundedness (L^∞) can be achieved in a straightforward manner. The unilateral control design is recoverable in the limit from the folding control design; therefore, the design is far more flexible as a methodology.

Without explicit solutions to the gain kernel equations, the effect of the design parameters on system response is difficult to quantify. However, numerical analysis is given which suggests at least qualitative intuition for selecting folding points for desired behavior. A waterbed effect is noted, in which the controller energy (L^2) exhibits an inherent trade off with boundedness (L^∞).

The observer utilized is a simple extension to the classical backstepping observer, where we have exploited the use of a collocated measurement somewhere within the interior of the system to generate decoupled classical backstepping observer problems. The cost of using this simplified approach is found in necessitating two measurements in the state and spatial derivative collocated at a single interior point.

The folding approach also opens the door to potential results involving 1-D PDEs exhibiting coupling structures at points on the interior, as opposed to spatially distributed coupling or boundary coupling. An extension to the folding framework, involving an unstable ODE coupled on an arbitrary point on the interior, is explored in [7]. Certainly, one may begin to

explore additional couplings, which involve feedback coupling between the unstable ODE and the parabolic PDE, or even coupling other 1-D PDEs at the boundary.

REFERENCES

[1] Y. Achdou, J. B. Francisco, J. Lasry, P. Lions, and B. Moll, "Partial differential equation models in macroeconomics," *Philosophical Transactions of the Royal Society A: Mathematical, Physical and Engineering Sciences*, vol. 372, no. 2028, Nov 2014.

[2] J. Auriol and F. Di Meglio, "Two-sided boundary stabilization of heterodirectional linear coupled hyperbolic PDEs," *IEEE Transactions on Automatic Control*, vol. 63, no. 8, pp. 2421–2436, 2018.

[3] A. Baccoli and A. Pisano, "Anticollocated backstepping observer design for a class of coupled reaction-diffusion PDEs," *Journal of Control Science and Engineering*, vol. 2015, p. 53, 2015.

[4] N. Bekiaris-Liberis and R. Vazquez, "Nonlinear Bilateral Output-Feedback Control for a Class of Viscous Hamilton-Jacobi PDEs," *ArXiv e-prints*, Mar. 2018.

[5] L. Camacho-Solorio, R. Vazquez, and M. Krstic, "Boundary observer design for coupled reaction-diffusion systems with spatially-varying reaction," in *2017 American Control Conference (ACC)*, May 2017, pp. 3159–3164.

[6] M. Chaplain, S. McDougall, and A. Anderson, "Mathematical modeling of tumor-induced angiogenesis," *Annual Review of Biomedical Engineering*, vol. 8, no. 1, pp. 233–257, 2006, pMID: 16834556. [Online]. Available: https://doi.org/10.1146/annurev.bioeng.8.061505.095807

[7] S. Chen, R. Vazquez, and M. Krstic, "Bilateral boundary control design for a cascaded diffusion-ode system coupled at an arbitrary interior point," *arXiv preprint: https://arxiv.org/abs/1906.04919*, 2019.

[8] G. A. de Andrade, R. Vazquez, and D. J. Pagano, "Backstepping stabilization of a linearized ode–pde rijke tube model," *Automatica*, vol. 96, pp. 98 – 109, 2018.

[9] J. Deutscher and S. Kerschbaum, "Backstepping control of coupled linear parabolic PIDEs with spatially varying coefficients," *IEEE Transactions on Automatic Control*, vol. 63, no. 12, pp. 4218–4233, 2018.

[10] L. Evans, *Partial Differential Equations*. American Mathematical Society, 1998.

[11] G. Freudenthaler, F. Göttsch, and T. Meurer, "Backstepping-based extended luenberger observer design for a burgers-type pde for multi-agent deployment," *IFAC-PapersOnLine*, vol. 50, no. 1, pp. 6780 – 6785, 2017, 20th IFAC World Congress. [Online]. Available: http://www.sciencedirect.com/science/article/pii/S2405896317316956

[12] A. Hastings, "Global stability in Lotka-Volterra systems with diffusion," *Journal of Mathematical Biology*, vol. 6, no. 2, pp. 163–168, Jul 1978. [Online]. Available: https://doi.org/10.1007/BF02450786

[13] M. Krstic and A. Smyshlyaev, *Boundary Control of PDEs: A Course on Backstepping Designs*. SIAM, 2008.

[14] Y. Orlov, A. Pisano, A. Pilloni, and E. Usai, "Output feedback stabilization of coupled reaction-diffusion processes with constant parameters," *SIAM Journal on Control and Optimization*, vol. 55, no. 6, pp. 4112–4155, 2017. [Online]. Available: https://doi.org/10.1137/15M1034325

[15] A. Smyshlyaev and M. Krstic, "Backstepping observers for a class of parabolic PDEs," *Systems & Control Letters*, vol. 54, no. 7, pp. 613 – 625, 2005. [Online]. Available: http://www.sciencedirect.com/science/article/pii/S0167691104001963

[16] ——, "On control design for PDEs with space-dependent diffusivity and time-dependent reactivity," *Automatica*, vol. 41, pp. 1601–1608, 2005.

[17] D. Tsubakino and S. Hara, "Backstepping observer design for parabolic PDEs with measurement of weighted spatial averages," *Automatica*, vol. 53, 03 2015.

[18] D. Tsubakino, M. Krstic, and Y. Yamashita, "Boundary control of a cascade of two parabolic PDEs with different diffusion coefficients," in *Decision and Control (CDC), 2013 IEEE 52nd Annual Conference on*. IEEE, 2013, pp. 3720–3725.

[19] J. Vázquez, *The porous medium equation: mathematical theory*. Oxford University Press, 2007.

[20] R. Vazquez and M. Krstic, "Bilateral boundary control of one-dimensional first- and second-order PDEs using infinite-dimensional backstepping," in *2016 IEEE 55th Conference on Decision and Control (CDC)*, Dec 2016, pp. 537–542.

[21] ——, "Boundary control and estimation of reaction–diffusion equations on the sphere under revolution symmetry conditions," *International Journal of Control*, pp. 1–10, 2017.

[22] ——, "Boundary control of coupled reaction-advection-diffusion systems with spatially-varying coefficients," *IEEE Transactions on Automatic Control*, vol. 62, no. 4, pp. 2026–2033, April 2017.

[23] S. Wang and F. Woittennek, "Backstepping-method for parabolic systems with in-domain actuation," *IFAC Proceedings Volumes*, vol. 46, no. 26, pp. 43–48, 2013.

[24] F. Woittennek, S. Wang, and T. Knüppel, "Backstepping design for parabolic systems with in-domain actuation and robin boundary conditions," *IFAC Proceedings Volumes*, vol. 47, no. 3, pp. 5175–5180, 2014.

Stephen Chen (S'13) received the B.S. degree in electrical engineering and computer sciences from the University of California, Berkeley, and the M.S. and Ph.D. degrees in mechanical engineering from the University of California, San Diego. He is currently a Senior Member of Technical Staff at the Charles Stark Draper Laboratory in Cambridge, Massachusetts. He has previously held internship positions with Tesla Motors in 2012, and ASML in 2016. His research interests include control theory, distributed parameter systems, partial differential equations, and optimization.

Rafael Vazquez (S'05-M'08-SM'15) received the electrical engineering and mathematics degrees from the University of Seville, Seville, Spain, and the M.S. and Ph.D. degrees in aerospace engineering from the University of California, San Diego. He is currently an Associate Professor in the Aerospace Engineering Department, University of Seville. His research interests include control theory, distributed parameter systems, and optimization, with applications to flow control, ATM, UAVs, and orbital mechanics. He is coauthor of the book Control of Turbulent and Magnetohydrodynamic Channel Flows (Basel, Switzerland: Birkhauser, 2007). Dr. Vazquez currently serves as Associate Editor for Automatica.

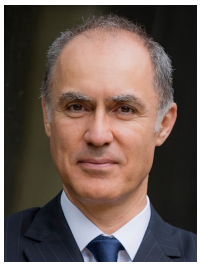

Miroslav Krstic (S'92-M'95-SM'99-F'02) holds the Alspach endowed chair and is the founding director of the Cymer Center for Control Systems and Dynamics at UC San Diego. He also serves as Associate Vice Chancellor for Research at UCSD. As a graduate student, Krstic won the UC Santa Barbara best dissertation award and student best paper awards at CDC and ACC. Krstic is Fellow of IEEE, IFAC, ASME, SIAM, and IET (UK), Associate Fellow of AIAA, and foreign member of the Academy of Engineering of Serbia. He has received the PECASE, NSF Career, and ONR Young Investigator awards, the Axelby and Schuck paper prizes, the Chestnut textbook prize, the ASME Nyquist Lecture Prize, and the first UCSD Research Award given to an engineer. Krstic has also been awarded the Springer Visiting Professorship at UC Berkeley, the Distinguished Visiting Fellowship of the Royal Academy of Engineering, the Invitation Fellowship of the Japan Society for the Promotion of Science, and the Honorary Professorships from the Northeastern University (Shenyang) and the Chongqing University, China. He serves as Senior Editor in IEEE Transactions on Automatic Control and Automatica, as editor of two Springer book series, and has served as Vice President for Technical Activities of the IEEE Control Systems Society and as chair of the IEEE CSS Fellow Committee. Krstic has coauthored eleven books on adaptive, nonlinear, and stochastic control, extremum seeking, control of PDE systems including turbulent flows, and control of delay systems.